

Comparison of the Impact Response of the THUMS Human Body Model and of the WorldSID Finite Element Model in Far Side Sled Tests

Shigeki Hayashi, Hiroshi Miyazaki, Kazuo Imura, Jakub Galazka, Andrea Lucchini-Gilera

Abstract In virtual testing for future assessments, it is expected future transition from a dummy use to human body model use or both. It is necessary to understand the differences of impact response and injury prediction between dummy and human body model. A far side sled model was generated using WorldSID model and THUMS version 4.1. Using pulses of Pole and Advanced European Mobile Deformable Barrier impacts defined in European New Car Assessment Programme far side protocol, simulations were performed on various conditions with the impact angles as parameter. WorldSID and THUMS head movement and rib fracture risk were predicted. The results showed that the THUMS head moved laterally about 100 mm more than the WorldSID head in all cases. WorldSID showed a low risk of rib fracture for both adult and elderly occupants. On the other hand, THUMS showed a low risk of injury for the adult occupant, but a high risk of rib fracture for the elderly occupant. The reason why the amount of movement of the head of THUMS is larger than that of WorldSID is because of larger amount of movement of the pelvis and upper torso caused by the soft flesh around the pelvis and flexible thoracic spine.

Keywords Chest injury risk, far-side sled simulation, human body FE model, WorldSID FE model.

I. INTRODUCTION

The European New Car Assessment Programme (Euro NCAP) introduced the far side impact test in the programme from the 2020 protocol [1]. Furthermore, Euro NCAP has decided the introduction of virtual testing from 2024 for the purpose of evaluating safety in various crash impact conditions [2]. According to the accident field data analysis conducted by [3] chest injury is the most frequent part in the serious injury (Abbreviated Injury Scale (AIS3+)). And in moderate injury (AIS2+), the chest injury is the second part contributor followed by the head/face/neck part. It is important to reduce the chest injury in the occurrence of far-side impact. Reference [4] reported the results of a study on model validation for a far side computer aided engineering model (CAE) used for a draft of virtual testing protocol. The validation criteria of the far-side sled model were discussed considering ISO TS18571 for the head, thoracic and pelvis responses of Worldwide Side Impact dummy (WorldSID). Different load cases to cover various conditions such as impact angle from 60° to 90° and seat cushion positions lowest and highest were proposed. It can be assumed that virtual testing implementation will only accelerate from the first application, since Euro NCAP has already announced the introduction of human body model (HBM) use in its 2030 road map [5]. In virtual testing for future assessments, it is expected to make, at some point, the transition from a dummy use to HBM use or both. It is necessary to understand impact response and biofidelity of WorldSID and HBM in far side environment. Several researchers conducted experimental study using WorldSID in far side environment. Reference [6] studied countermeasures such as shoulder, thorax plate and inboard shoulder belt for far side occupant. Those countermeasures effectiveness to reduce head excursion, injury risks of lower neck or chest were pointed out. In a series of far side experiments, Reference [7] conducted a comparison of post mortem human subjects (PMHS), WorldSID and a test device for human occupant restraint dummy (THOR) responses. WorldSID is more biofidelic than THOR in various far side impact conditions. Due to the rib deflection sensor location, difficulty of prediction of chest injury was indicated in this study. References [8-10] compared WorldSID and PMHS kinematics in far side impact experiment. The result showed a good agreement between WorldSID and PMHS head lateral excursion. However, increase of impact velocity (16 to 34 km/h) and addition of pelvis restraint had an effect of making PMHS head excursion larger than WorldSID. And also it was pointed out

S. Hayashi (shigeki_hayashi_aa@mail.toyota.co.jp; 81-50-3165-5346) is Project Manager, K. Imura is Group Manager, H. Miyazaki is Assistant Manager in Toyota Motor Corporation, Japan. J. Galazka is Senior Engineer and A. Lucchini-Gilera is Senior Manager in Toyota Motor Europe, Belgium.

that WorldSID rib deflection measurement does not represent the rib fracture mechanisms generated by anterior loading from seat belt due to its rib structure and sensor location. Human body models were compared with PMHS in far side impact environments. Reference [11] compared the simplified Global Human Body Models Consortium's model (GHBMC) and PMHS. The morphed GHBMC to the PMHS size showed a good agreement with PMHS kinematics. It was indicated that the shoulder belt engagement was a key for kinematics and soft tissue deformation seemed to have an effect on body kinematics. Reference [12] conducted a comparative verification of the kinematics of PMHS and the SAFER-HBM with and without frontal centre airbag (FCAB) in a vehicle-based set-up including seat, console and belt. Even though the HBM predicted larger head excursion than PMHS in both with and without the airbag, it was confirmed that the HBM shows the benefit of safety countermeasure. Authors, in a previous study [13], used a modified Total Human Model for Safety (THUMS) version 4.1 to compare PMHS kinematics and rib fracture prediction in the far side environment demonstrated by [14]. The head movements predicted for the lateral and vertical directions were matching the corridor obtained by the PMHSs. In addition, THUMS, which had adjusted rib cortical bone thickness and material properties, corresponding to the average age of the PMHS, predicted the same number of rib fractures and locations.

The objective of this study is to compare the HBM THUMS and the WorldSID Finite Element Model considering kinematics and impact responses during far side impact, including vehicle interior environment. Chest injury risk predicted by both the models were also compared.

II. METHODS

In this study, simulations were performed using LS-DYNA code Version 971 R11 solver.

WorldSID Model Validation

An in-house WorldSID model was used. The model qualifies to the International Organization for Standardization (ISO) 15830 (External Measurement, Mass, Range of motion, Sensors, dummy dynamic qualification procedures) [15]. Following the ISO15830 requirements, validation of the whole body impact response in the environment of the far-side impact was conducted. Target validation data were selected from far-side sled test results using WorldSID conducted by [14] and [16]. Impact velocity were 11 m/s for [14] and 8 m/s for [16], respectively. Both projects used the same sled environment consisting of a rigid seat, footrest, centre console, 3-point seat belt and retractor. A static pretension was applied to the belt near the retractor outlet. Figure 1 shows the far side sled model used for the WorldSID model validation. For these tests, not only the WorldSID sensor measurements, but also belt forces and contact forces were measured as the main restraint forces of the dummy. For the absolute comparison of the dummy sensors, belt and console forces between test result and validation CAE, ISO18571 were used [17]. Weighted sensor ISO values are derived from Equation (1) as below. This equation was proposed Euro NCAP-Virtual Testing for Crash activity (Euro NCAP VTC)[4] and aims to not emphasise a small output polarity in a non-impact direction.



Fig. 1. In-house WorldSID model in the far side environment [14][16].

$$ISO_{Sensor} = \frac{abs \max(Sensor_x) \cdot ISO_{Sensor_x} + abs \max(Sensor_y) \cdot ISO_{Sensor_y} + abs \max(Sensor_z) \cdot ISO_{Sensor_z}}{abs \max(Sensor_x) + abs \max(Sensor_y) + abs \max(Sensor_z)} \quad (1)$$

where, $abs \max(Sensor_x)$: Absolute maximum value of x-direction sensor
 $abs \max(Sensor_y)$: Absolute maximum value of y-direction sensor

$abs\ max(Sensor_z)$: Absolute maximum value of z-direction sensor
 ISO_{Sensor_x} : ISO score of x-direction sensor
 ISO_{Sensor_y} : ISO score of y-direction sensor
 ISO_{Sensor_z} : ISO score of z-direction sensor

THUMS and Chest Injury Prediction

In a previous study [13], THUMS Version 4.1 and its modified version were validated by comparing with the PMHS response in the far side experiment conducted by [14]. Stiffening of the neck muscles, scaling cortical bone stress-strain curve and thickness of the ribs, sternum and clavicles were introduced in THUMS 4.1 as a modified version to adjust the target age of the PMHSs tested. Both THUMS models kinematics resembled the PMHSs overall kinematics, however for the rib fracture prediction, the modified THUMS gave a prediction more in line with the PMHSs rib fracture number due to age influence.

In this study, three types of THUMS (original 35 years old (YO), 45YO and 67YO) were prepared for comparison with WorldSID which has chest injury risk curves of 45YO and 67YO [18]. Yield stress of rib, sternum and clavicle cortical bones were decreased from 80 MPa (35YO) to 79 MPa (47YO) and 74 MPa (67YO), failure plastic strain from 2.04 % (35YO) to 1.91 % (47YO) and 1.24 % (67YO) and the thorax cortical bone thickness was decreased by 7.2% (47YO) and 23.2% (67YO) from THUMS V4.1 (35YO) as shown in Fig.2. The rib fracture of three type THUMSs were predicted by the failure plastic strain. The neck muscle modification was introduced to all THUMSs based on the previous study as shown in Figure 3.

Injury values of the THUMS were estimated for the comparison with the WorldSID. Neck force and moment of THUMS were measured at cross-section C1 for the upper neck and C7 for the lower neck. Lumbar force and moment of THUMS were measured at cross-section L3. Chest deflection of THUMS was obtained by measuring the reduction in distance from a node on the outermost side of each rib to a virtual centre plane from the spine. Corresponding rib and spine for chest deflections were rib 6 and T6 for upper chest, rib 8 and T8 for middle chest, rib 9 and T9 for lower chest. Corresponding measured points for abdominal deflections were the tip of rib 10 and L2, inner surface of abdomen and L4.

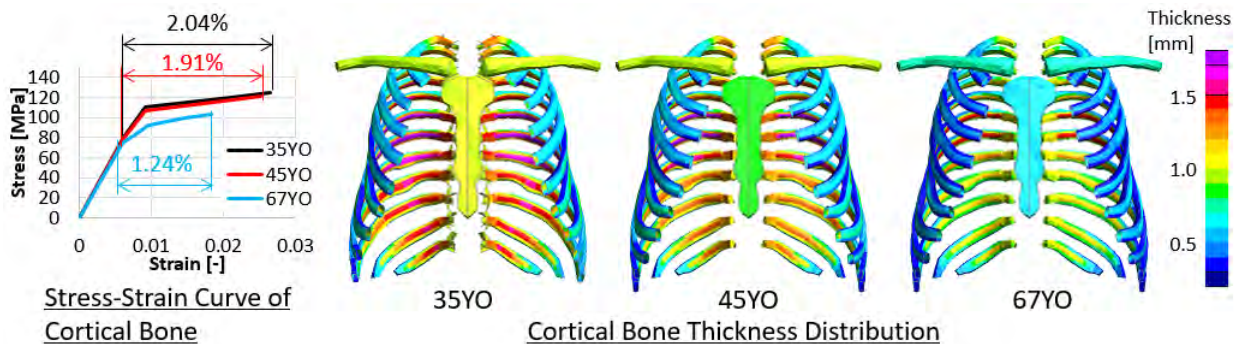


Fig. 2. Rib sternum and clavicle age related modification.

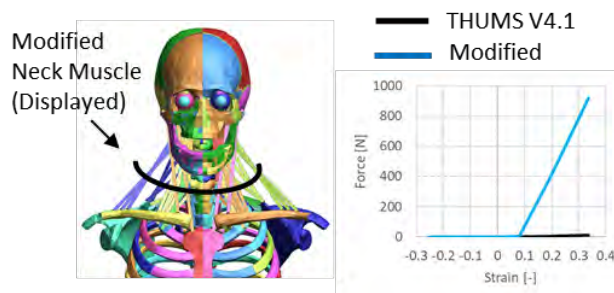


Fig. 3. Neck muscle modification.

Far Side Sled Model

A total of 16 simulations were conducted as listed in Table I. In house far side sled tests were performed to validate the sled model in terms of the body kinematics and injury response of the WorldSID. THUMS described

in the previous section was used for the comparison with the WorldSID in terms of body kinematics, injury response and interaction between vehicle interior parts. A sled model of sport utility vehicle was prepared for the far side impact simulations including the body shell and the interior parts that may contact the occupant, such as seats, seatbelt and centre console as shown in Figure 4. The width of centre console was 210 mm. And height of the centre console to top surface from the occupant hip point was 193 mm. The seat belt has 5% elongation at 11.1 kN force applied. The pre-tensioner was modelled by energy time history, so that belt force estimation could meet various impact conditions. The belt force limiter (4kN) was installed. The WorldSID dummy model posture was adjusted to the measured points at the test such as the hip point, head center of gravity, shoulder point and neck bracket. Then the dummy jacket fitting to the posture was simulated. Final seating simulation adjustment were to move the hip point to the target position of test by using "Boundary Prescribed Motion". Seat belt fitting was also conducted to set to test condition. The deformed seat and dummy fresh form had pre-stressed by defining "Initial Reference Geometry". The frictions were defined as 0.4, 0.5 and 0.2 between the dummy and seat, belt and centre console respectively. The same steps were conducted to THUMS seating simulations. The passenger seat frame was constrained by inserting foam blocks in between the B-pillar and centre console as described in Euro NCAP *FAR SIDE OCCUPANT TEST & ASSESSMENT PROCEDURE* [1]. The far side airbag was not used in this study. The sled body in the tests was accelerated up to 11.7 m/s derived from a 32 km/h Pole impact and 9.8 m/s derived from a 60 km/h Advanced European Mobile Deformable Barrier face (AEMDB) impact of a mid-sport utility vehicle (SUV) as shown in Figure 4. The sled body formed angles at 60°, 75° and 90° with the sled travel axis (Y-axis). In the meantime, the sled CAE model was fixed at 90° with the sled body longitudinal centreline (x-axis). And the pulse vectors were defined with directional components of 60°, 75° and 90° (X-axis component: Pulse times cos(angle)), Y-axis component: Pulse times sin(angle)). The impact angle was selected referring to the information of Euro NCAP VTC [4]. Adjustable seat height was set at the lowest most in all impact cases. Seat belt pre-tensioner was triggered at 9 ms. Even if belt force limiter (4kN) was installed, belt force did not reach the threshold force in the series of tests. Head kinematics of the WorldSID in the tests were calculated using its head G and angular velocity sensors. The CAE data of the head kinematics were derived from the result of the head center of gravity with respect to the vehicle coordinates.

TABLE I
TEST AND SIMULATION MATRIX

Case	Occupant	Pulse	Impact Angle (degrees)	Test for Model Validation	CAE
1	WorldSID	Pole	60	✓	✓
2			75	✓	✓
3			90	✓	✓
4		AEMDB	75	✓	✓
5	THUMS 35YO with neck modification	Pole	60		✓
6			75		✓
7			90		✓
8		AEMDB	75		✓
9	THUMS 45YO with neck modification	Pole	60		✓
10			75		✓
11			90		✓
12		AEMDB	75		✓
13	THUMS 67YO with neck modification	Pole	60		✓
14			75		✓
15			90		✓
16		AEMDB	75		✓

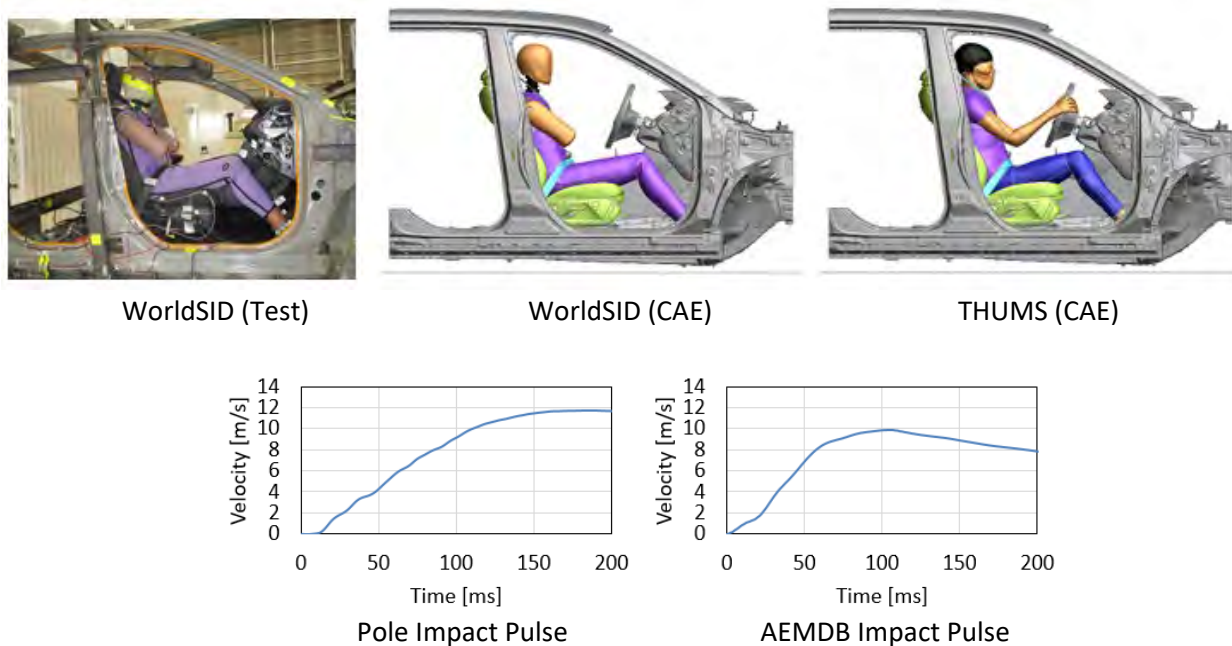


Fig. 4. Far side sled test and simulation models.

III. RESULTS

WorldSID Model Validation

Figure 5 shows the head kinematics. In 8 m/s load case, lateral excursion of the head was 580 mm in the test and 540 mm in CAE, consequently in 11 m/s load case 679 mm in the test and 676 mm in CAE. Deviation between test and CAE in terms of head excursion were 7.4% and 0.4% respectively (Table II). The result of weighted sensor ISO values derived from Equation (1) are listed for both cases in Table III. Time history of kinematic and internal load channels for 8 m/s and 11 m/s are shown in Appendix A1 and A2. Averaged ISO values were bigger than 0.6 which is defined as threshold of model validation in the draft of virtual testing protocol [4].

Overall, the WorldSID model appeared to be capable of predicting the impact response in far side impact.

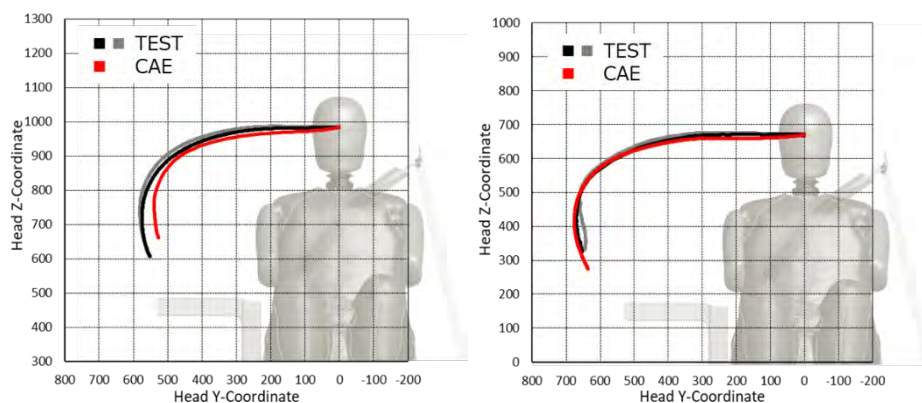


Fig. 5. Head kinematics (Left 8 m/s, Right 11 m/s).

TABLE II
HEAD LATERAL MOVEMENT COMPARISON

Velocity	Test	CAE	Deviation
8 m/s	580 mm	540 mm	7.4 %
	575 mm		6.5 %
11 m/s	679 mm	676 mm	0.4 %
	664 mm		1.8 %

TABLE III
ISO Value

Load case		OSSCAR 8 m/s	CESSAR 11 m/s
Interval of Evaluation		t=0.04-0.18s	t=0.03-0.15s
Kinematics	Head Angular Velocity	0.735	0.763
	Head Acceleration	0.734	0.756
	T1 Acceleration	0.672	0.646
	T12 Acceleration	0.746	0.680
	Pelvis Acceleration	0.713	0.647
Internal loads	Upper Neck Force	0.737	0.782
	Upper Neck Moment	0.637	0.630
	Lumbar Force	0.563	0.719
	Lumbar Moment	0.672	0.475
	Abdomen Rib Deflection	0.802	0.742
Average		0.701	0.684

Far Side Sled Model Validation

Figure 6 shows the WorldSID kinematics in the Pole 75° impact case. The dummy upper torso moved sideways and the lower chest contacts the centre console while the pelvis is restrained by the lap belt. The shoulder belt slips off the shoulder at approx. 100 ms. These observations were confirmed in the CAE model.

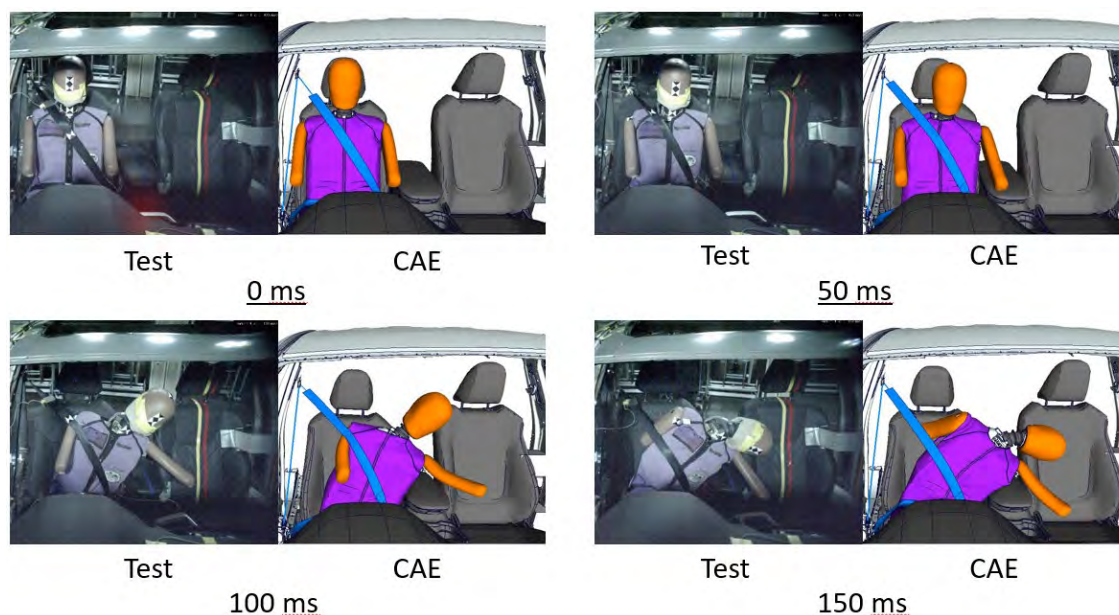


Fig. 6. Far side sled test and simulation model in Pole 75°.

Head kinematics are described in Figure 7 comparing test and CAE. The result shows in both tests and CAE, that initially the head moves in the lateral and downward direction. As the head approaches the maximum lateral displacement, the head is likely to move more downward due to its rotation around neck. Deviation of the head lateral movement between the test and CAE ranged from 4.8% to 12.7%.



Fig. 7. Head kinematics comparison.

Figure 8 shows the head, thoracic spine (T12) and pelvis response vs time history in the case of the Pole 75° impact. The data were filtered with CFC60. Peak G timing in the lateral direction (GY) was first reached at the pelvis (70 ms) and then at T12 after an additional 10 ms. The peak head acceleration in vertical direction (GZ) was observed at 120 ms. The peak head GY occurred at around 150 ms which coincided with the timing of most head lateral movement. The entire trend of CAE estimation coincided with the test results described above. ISO scores were calculated for the channels according to ISO/DTS 18571 standard [17] to make absolute comparison between test and CAE. GY and GZ channels scored a range from 0.547 to 0.815, while the longitudinal direction (GX) channel received relatively low scores from 0.252 to 0.444. Since GX sensor outputs were relatively lower due to the lateral impact conditions, higher model prediction performance in longitudinal is required to obtain higher ISO values.

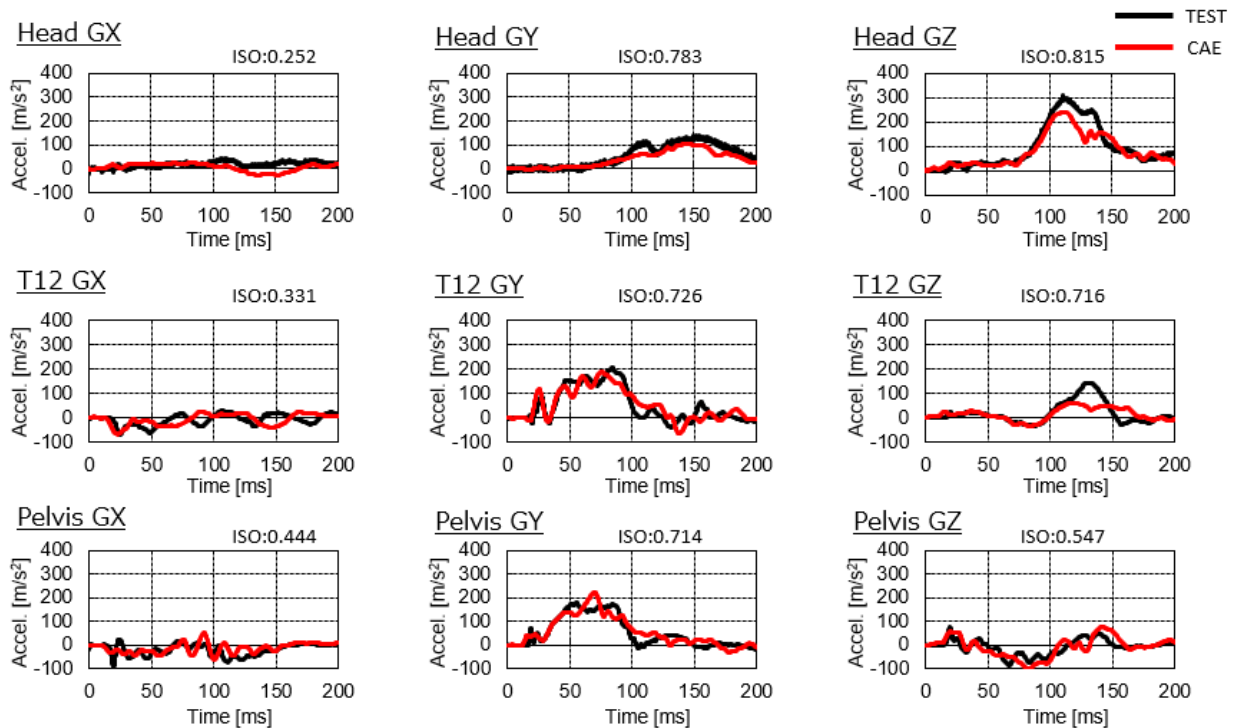


Fig. 8. Comparison of G response of the Head, Thoracic spine (T12) and Pelvis.

The weighted ISO scores of load cases are described in Figure 9. The highest ISO was 0.81 at head G in the Pole 90° while the lowest ISO was 0.58 at pelvis G in the Pole 90°.

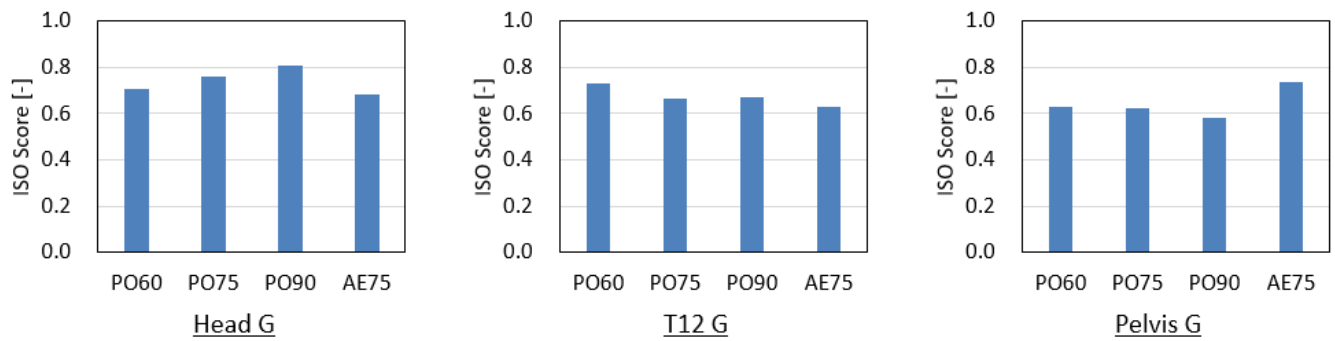


Fig. 9. Weighted ISO values in G response of Head, Thoracic spine (T12) and Pelvis.

Injury values of the test results and the CAE estimation were compared (see Appendix B1). The values were calculated using the filter class defined in the Euro NCAP Technical Bulletin (TB021) [19]. The dotted lines in the graphs are low thresholds defined in the protocol. Lower neck lateral moment (MX) of both test and CAE is close to the threshold, but other injuries are relatively lower than each threshold. CAE injury estimation generally matched the test result except neck moment (MY). This is due to the lower prediction performance of the model in our study as shown in the low ISO value of the head and chest GX in Figure 8.

Comparison of Occupant Kinematics

Figure 10 shows the occupant kinematics comparison between WorldSID (red line) and THUMS (blue line) of the head, T1, T12 and pelvis in a front view at the time when the head reached the maximum lateral movement with respect to the sled body for Pole 75°, in addition the front view of WorldSID and THUMS, respectively, at the time when the head reached maximum lateral movement is shown. The actual values of displacements for all cases are listed in Table IV. The other kinematics comparison and front view of Pole 60°, 90° and AEMDB 75° are shown in Appendix C1. Overall, WorldSID and THUMS showed similar kinematics. The following were observed in all impact cases: 1) The pelvis was constrained mainly by the belt and not so strong contact with console was observed. After maximum lateral movement, upward and outside rebound was observed; 2) Chest contact with the console was observed. T12 rebounds upward after console contact as the head moves downward; 3) The right shoulder slipped off from the shoulder belt; and 4) The head translated not only laterally in the initial phase, but also downward movement was observed. The largest head movement was observed in Pole 90° followed by Pole 75°, AEMDB 75° and Pole 60°. The most relevant different points between WorldSID and THUMS include: 1) THUMS pelvis moved more laterally and rotated more than WorldSID; 2) THUMS lower chest contacted with the console while WorldSID middle chest contacted with the console; 3) THUMS head moved more laterally around 100mm than WorldSID; and 4) The most bended location in the spine of THUMS was the neck but the chest and lumbar spine also bent smoothly while the neck and lumbar spine were the only bending locations in WorldSID.



Fig. 10. Occupant kinematics comparison in Pole 75°.

TABLE IV
LATERAL MOVEMENT AT HEAD MAXIMUM TIME

Load case	Pole 60°		Pole 75°		Pole 90°		AEMDB 75°	
	WorldSID (155 ms)	THUMS (156 ms)	WorldSID (153 ms)	THUMS (147 ms)	WorldSID (150 ms)	THUMS (145ms)	WorldSID (128 ms)	THUMS (128 ms)
Head	469	566	537	637	545	664	533	625
T1	318	386	370	446	371	474	367	432
T12	108	142	121	165	115	172	105	148
Pelvis	23	73	29	86	39	88	61	66

Comparison of Contact Force

Figure 11 shows comparison of contact force (Y) between WorldSID and THUMS in the case of Pole 75°. The other comparison of Pole 60°, 90° and AEMDB 75° are shown in Appendix C2. Seat cushion force ranged from 1.5kN to 2 kN for both WorldSID and THUMS in all cases. Seat back force for both occupants increased gradually with the increase of the impact angle, 1kN at Pole 60°, 2 kN at Pole 75° and Pole 3 kN at Pole 90°. Shoulder seat belt force with THUMS was larger than that of WorldSID due to the interaction with the arm. However, as soon as the shoulder-belt interaction ceased due to the slip off, the shoulder belt force dropped at around 90 to 100 ms in Pole impacts and at 75 ms in AEMDB. Contact force between the hip and belt buckle was included in the lap belt force. Lap belt force ranged from 3 kN to 4 kN in Pole impacts and 5 kN in AEMDB. THUMS contact force in Pole 60° was 1kN higher than WorldSID. THUMS contact force rised slower and peaked later compared to WorldSID. Console force with WorldSID was concentrated to chest lower in Pole impact and abdomen in AEMDB, while console force was distributed from chest to abdomen of THUMS in all cases.

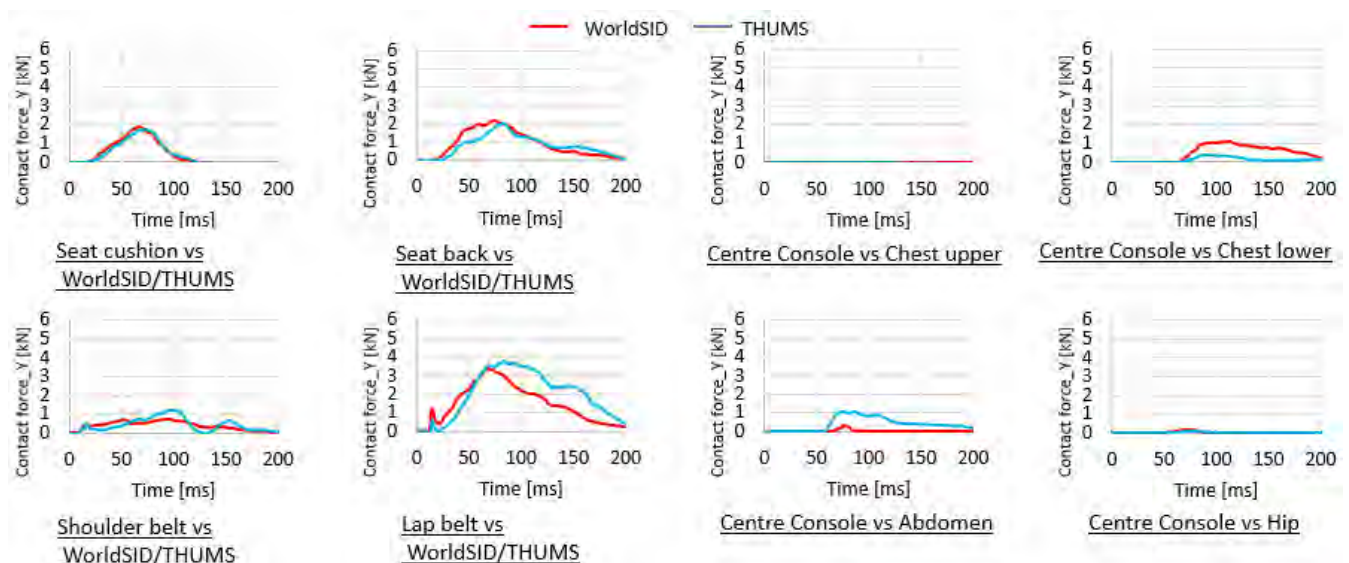


Fig. 11. Contact force (Y) comparison in Pole 75°.

Comparison of Injury Value

Estimated injury values are shown in Figure 12 for the head, neck, lumbar, pubic and deflection of chest and abdomen in the case of Pole 75°. The Euro NCAP higher thresholds are plotted as dotted line for reference.

Head injury (HIC and 3msG) response in WorldSID and THUMS are similar. The head injury values increased with increasing impact angle in the Pole for both models. A big difference was observed in neck and lumbar responses between WorldSID and THUMS. Tension and moment of WorldSID neck and lumbar were 3 to 4 times bigger than THUMS's, whereas lumbar shear force values were the same level between WorldSID and THUMS. Regarding the chest and abdominal deflections, WorldSID rib deflected mainly at the middle and lower chest while THUMS deflections generated at the lower chest and upper abdomen. This could be explained by the

different contact to centre console kinematics inducing different interactions and loading of ribs between WorldSID and THUMS.

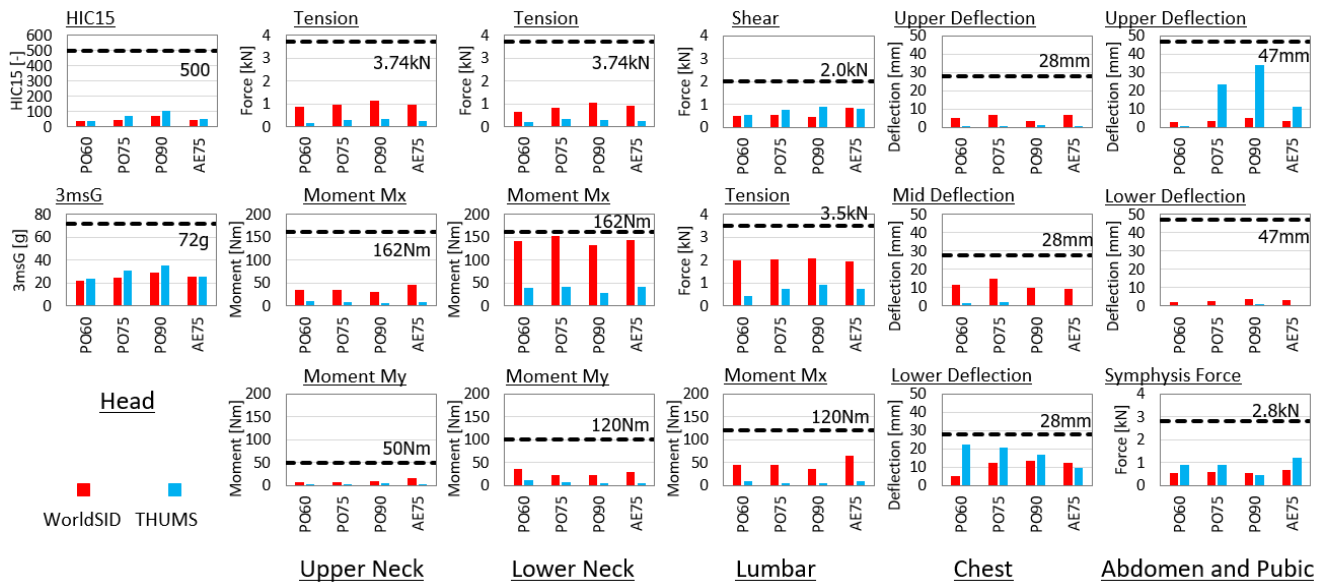


Fig. 12. Comparison of Injury Values between WorldSID and THUMS.

Comparison of Injury Prediction

Figure 13 shows thoracic injury risk prediction AIS3+ of WorldSID and number of rib fracture of THUMS. The risk curves of WorldSID were referred to ISO [12]. The location of rib fracture of THUMS is shown in Appendix D. WorldSID thoracic skeletal risks of all cases were zero for the 45 YO and the 67 YO occupants. On the other hand, THUMS predicted more than three rib fractures for the 67 YO occupant in all cases. Two or three rib fractures for the 45 YO occupant, and one rib fracture for the 35 YO occupant were predicted in Pole 75°, 90° and AEMDB 75° impact cases. All fractures were estimated at left lower chest due to the contact with the centre console. THUMS showed higher thoracic skeletal injury risk than WorldSID.

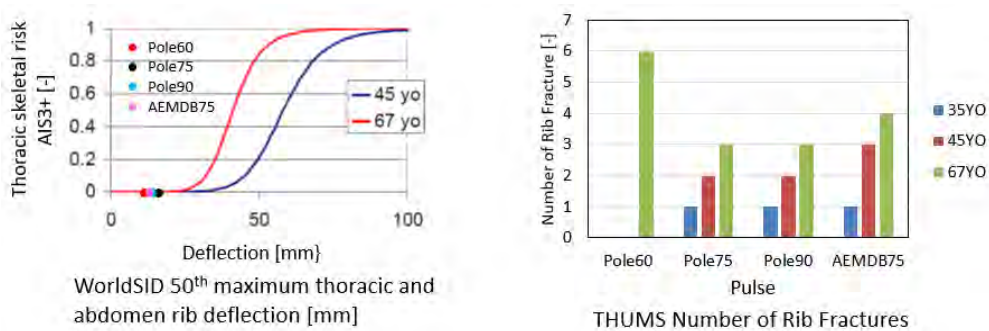


Fig. 13. Injury risk prediction of WorldSID and THUMS.

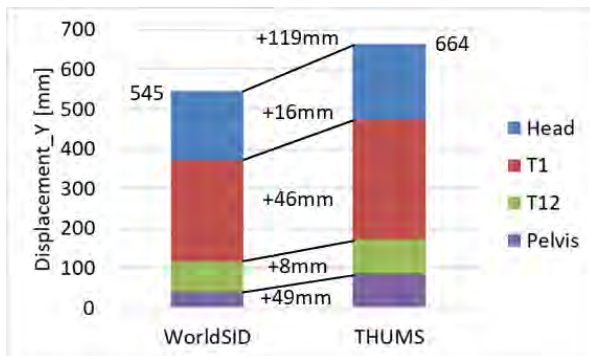
IV. DISCUSSION

The impact response of WorldSID and the human body model THUMS were compared in various Far side impact environments including impact angles of 60°, 75°, 90° Pole and of 75° AEMDB.

Head Excursion

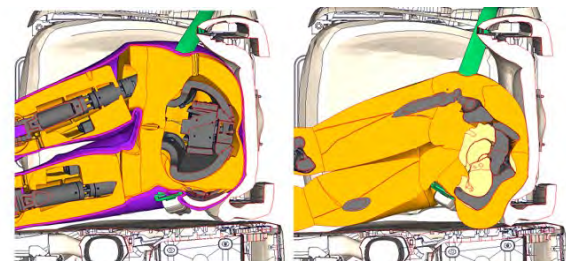
THUMS head lateral movement was about 100 mm greater than WorldSID in all cases. Figure 14 shows the comparison of the head lateral movement between WorldSID and THUMS based on the cumulative amount of the pelvis and spine (T12 and T1) in the case of Pole 90° which is the case where the highest lateral movement

difference was observed as 119 mm. The section cut views at the hip are also shown in the Figure 15. The big difference between WorldSID and THUMS was found in the pelvis movement and T1 movement. The differences are 49 mm in pelvis, and 46 mm in T1 (thoracic spine base), respectively. There is not such big difference in T12 (lumbar spine base) with 8 mm and the head (neck base) with 16 mm. This result can be explained by the rigid thoracic spine and soft lumbar spine structure of WorldSID. Next the reason of the pelvis movement difference between WorldSID and THUMS is discussed. The flesh around the pelvis of THUMS deformed and bottomed out due to the contact with the lap belt, while the flesh of WorldSID deformed less. It is presumed that the difference of flesh softness induced the large pelvis movement in THUMS compared to WorldSID.



Lateral movement of body region (Pole 90°)

Fig. 14. Comparison of Lateral movement of body region between WorldSID and THUMS.



WorldSID 150 ms THUMS 145 ms
Section view (Pole 90°)

At Head maximum displacement timing

Fig. 15. Comparison of the hip deformation between WorldSID and THUMS.

Injury Risk

WorldSID chest and abdomen in all cases showed a range from 1 to 15 mm deflection which is less than the higher thresholds, chest deflection is 28 mm and abdominal deflection is 47 mm, defined in the Euro NCAP protocol [1]. When the chest and abdominal deflections were applied to injury risk curves for the 45 YO and 67 YO, the thoracic skeletal risk AIS3+ was not expected (zero risk). However, when we looked at the THUMS rib fracture estimation, more than three rib fractures classified AIS3 were predicted for 67 YO. And one or two rib fractures were predicted for younger THUMS (35 YO and 47 YO). This underestimation of chest injury risk for WorldSID was discussed in the other research [9-10]. Since WorldSID chest/abdominal deflection sensors only measure purely lateral loading, frontal loading from shoulder belt to chest is not considered for the injury prediction. And biofidelity of chest responses against the frontal loadings have not been studied. In this study, the THUMS 67 YO in the Pole 60° predicted highest number of rib fractures (six). The belt contact X-force 3 kN to chest was also the highest compared to other impact directions (2 kN in Pole 75°, 1 kN in Pole 90°) while center console contact Y-force had same range of 4 kN in all impact cases. This indicated that frontal loading to chest from seat belt has great effect to chest injury. The THUMS rib fracture risk result is closer to the field accident data reported as high injured body region in AIS3+ [3]. Rib fractures were generated at the time of the contact with the centre console in the THUMS kinematic analysis. Assuming a smaller occupant, the hypothesis would be that the contact location of the chest to the console would move up to the chest upper area and cause higher injury risk since the upper chest moves laterally more than the lower chest. Indeed, the field data show that the smaller occupant is more likely to sustain chest injury [3]. To clarify the hypothesis, a study using a smaller size of HBM is required since a small occupant dummy having high biofidelity for far side impacts has not been substantiated.

The WorldSID neck and lumbar spine injury values in Figure 12 were higher than those of the THUMS. Stiffer spine of WorldSID made the difference. However, the field data [3] shows for spine injury even smaller numbers compared with chest injury. Research is required for spine injury assessment method and threshold using HBM for the coming virtual testing.

V. CONCLUSIONS

The impact response of WorldSID and the THUMS HBM was examined in a far side environment for considering the future introduction of an HBM in virtual testing. The in-house developed WorldSID model was validated in a generic far side sled condition at 8 m/s and 11 m/s.

The validity of a vehicle sled model was examined comparing tests and simulations in impact angles of 60°, 75°, 90° Pole pulse at 32 km/h and 75° AEMDB pulse at 60 km/h using the validated WorldSID model. THUMS was used in the validated vehicle sled model for the comparison with the WorldSID. With the limited and assumed impact conditions, the study found following conclusions through the simulations.

The THUMS head lateral movement was approx. 100 mm larger than the WorldSID model in all impact cases. The study found that the difference of head lateral movement between THUMS and WorldSID was due to the cumulative differences of greater pelvis movement 50 mm and thoracic spine bending 50 mm of THUMS. The soft flesh of the pelvis and flexible thoracic spine of THUMS induced the differences

The predicted maximum WorldSID chest rib deflection was 15 mm at Pole 75° impact among all cases, which was lower than the higher injury thresholds defined in the current Euro NCAP protocol [1] in all cases. Furthermore, the rib fracture risk of deflection 15 mm of AIS3+ was zero for the 47 YO and the 67 YO occupants at the definition of ISO risk curves. On the other hand, the THUMS predicted more than three rib fractures for the 67 YO occupant in all cases. The THUMS showed higher thoracic skeletal injury risk than the WorldSID.

VI. REFERENCES

- [1] Euro NCAP Far side occupant test & assessment procedure version 2.3, 2022, European New Car Assessment Programme
- [2] Euro NCAP 2025 Roadmap, <https://www.euroncap.com>
- [3] Klug C, Rudd R, Fitterer S, Tomasch E, Blume H, Craig M, Wernicke P. Priorities in Far-side Protection - What can we learn from field data for the development of virtual testing protocols? Proceedings of IRCOBI Conference, 2022, Porto, Portugal
- [4] Klug C, Schachner M, Ellway J, Eggers A, Galazka J, Gargallo S, Jimenez C, Kirch J, Levallois I, Lobenwein U, Meissner N, Pardede V, Pipkorn B, van Ratingen M. Euro NCAP Virtual Testing – Crashworthiness, Enhanced Safety of Vehicles, 2023, Yokohama, Japan.
- [5] Euro NCAP 2030 Roadmap, <https://www.euroncap.com>
- [6] Pintar F, Yoganandan N, et al. WORDSID ASSESSMENT OF FAR SIDE IMPACT COUNTERMEASURES, 50th Annual Proceedings Association for the Advancement of Automotive Medicine, October 16-18, 2006
- [7] Pintar F, Yoganandan N, et al. Comparison of PMHS, WorldSID, and THOR-NT Responses in Simulated Far Side Impact, Stapp Car Crash Journal, Vol. 51, October 2007, pp. 313-360
- [8] Perz-Rapela D, Markusic C, et al. Comparison of WorldSID to PMHS kinematics in far-side impact, Proceedings of IRCOBI Conference, 2018, Athens, Greece
- [9] Perz-Rapela D, Donlon J-P, et al. PMHS and WorldSID Kinematic and Injury Response in Far-side Events in a Vehicle-Based Test Environment, Stapp Car Crash Journal, Vol. 63, November 2019, pp. 83-126
- [10] Perz-Rapela D, Donlon J-P, et al. Occupant Restraint in Far-Side Impacts: Cadaveric and WorldSID Responses to a Far-Side Airbag, Annals of Biomedical Engineering, Vol. 49, No. 2, February 2021, pp. 802-811
- [11] Perz-Rapela D, Markusic C, Whitcomb B, Pipkorn B, Forman J, Crandall J, Comparison of the simplified GHBM to PMHS kinematics in far-side impact, Proceedings of IRCOBI Conference, 2019, Florence, Italy
- [12] Pipkorn B, Osth J, et al., Validation of the SAFER Human Body Model Kinematics in Far-Side Impacts, Proceedings of IRCOBI Conference, 2021, Munich, Germany.
- [13] Hayashi S, Miyazaki H, Kitagawa Y, Compigne S. Validation of THUMS Human Body Model in Far Side Impact, Proceedings of IRCOBI Conference, 2021, Munich, Germany.
- [14] Petit P, Trosseille X, Uriot J et al. Far side impact injury threshold recommendations based on 6 paired WorldSID / Post Mortem Human Subjects tests, Stapp Car Crash Journal, 2019, Vol. 63, 19S-23.
- [15] ISO, ISO/15830, Road vehicles – Design and performance specifications for the WorldSID 50th percentile male side-impact dummy-, 2005
- [16] Hamacher M, Becker J, D’Addetta G, Ostling M, Mayer C, Compigne S, Final virtual design of advanced passenger protection principles, OSCCAR: FUTURE OCCUPANT SAFETY FOR CRASHES IN CARS, D2.4, 2021
- [17] ISO, ISO/DTS18571, Road vehicles - Objective rating metric for non-ambiguous signals, ISO/TC 22/SC 36 “Safety and impact testing”, VOTE by 2022-12-09
- [18] ISO, ISO/TR 12350, Road vehicles - Injury risk curves for the evaluation of occupant protection in side impact tests, 2013.
- [19] Euro NCAP Technical Bulletin, TB021 - Data format and Injury Criteria Calculation Version 4.0.2, 2022, European New Car Assessment Programme.

VII. APPENDIX

A. WorldSID Model Validation

Target validation data were selected from far-side sled test results using WorldSID conducted by [14] and [16]. Impact velocity were 11 m/s for [14] and 8 m/s for [16], respectively.

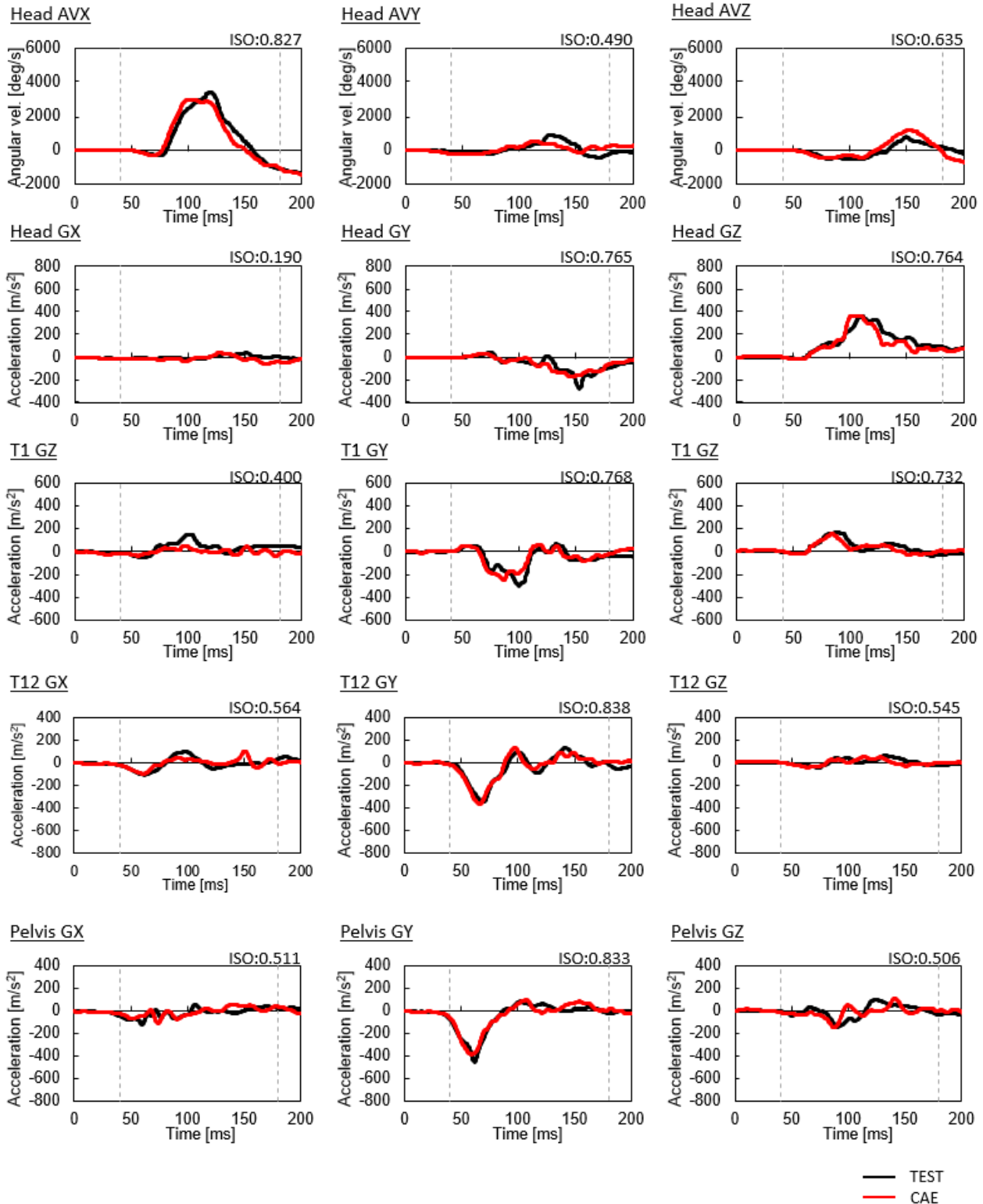


Fig. A1. Comparison of WorldSID time history sensor outputs (8 m/s).

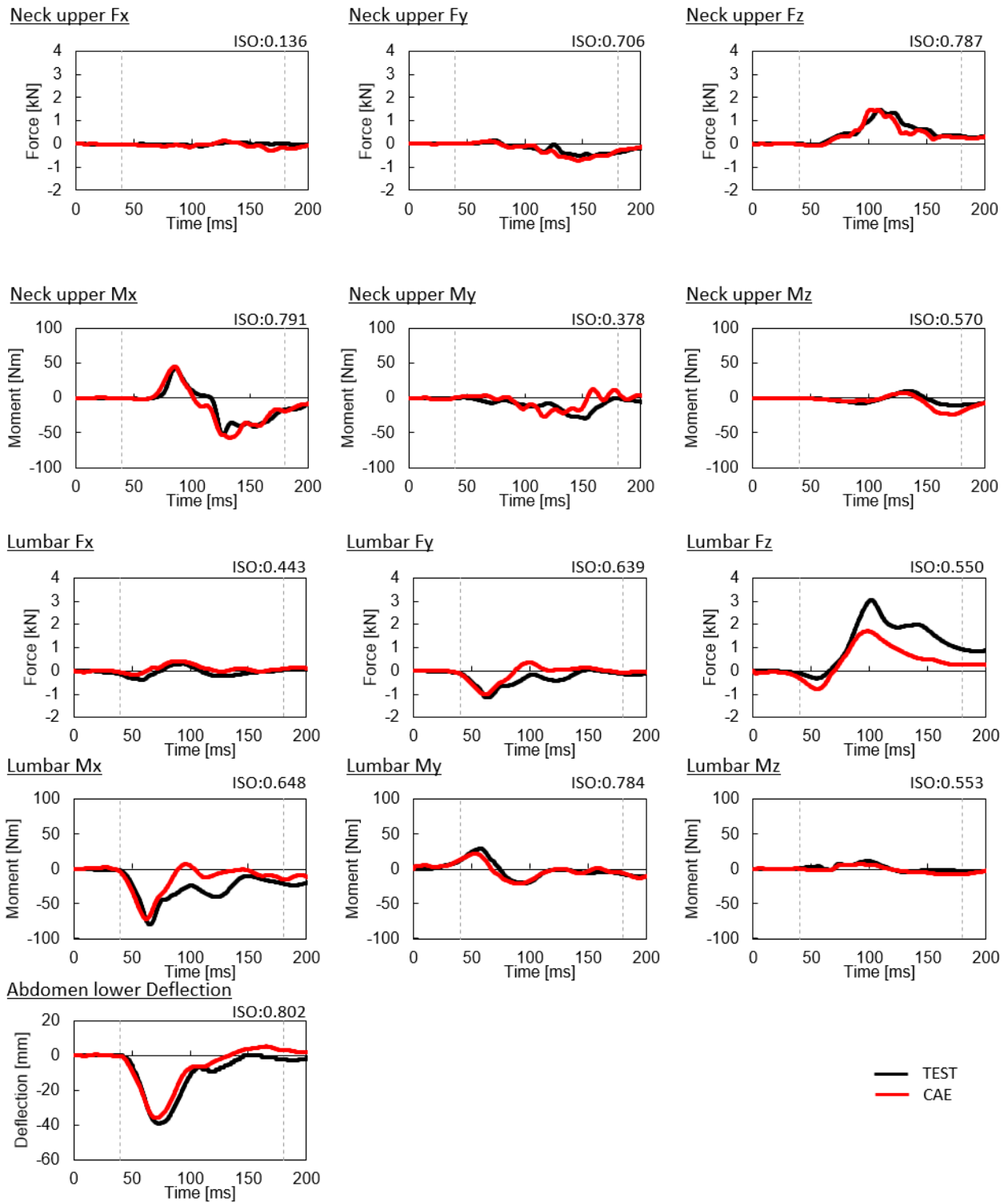


Fig. A1. Comparison of WorldSID time history sensor outputs (8 m/s).

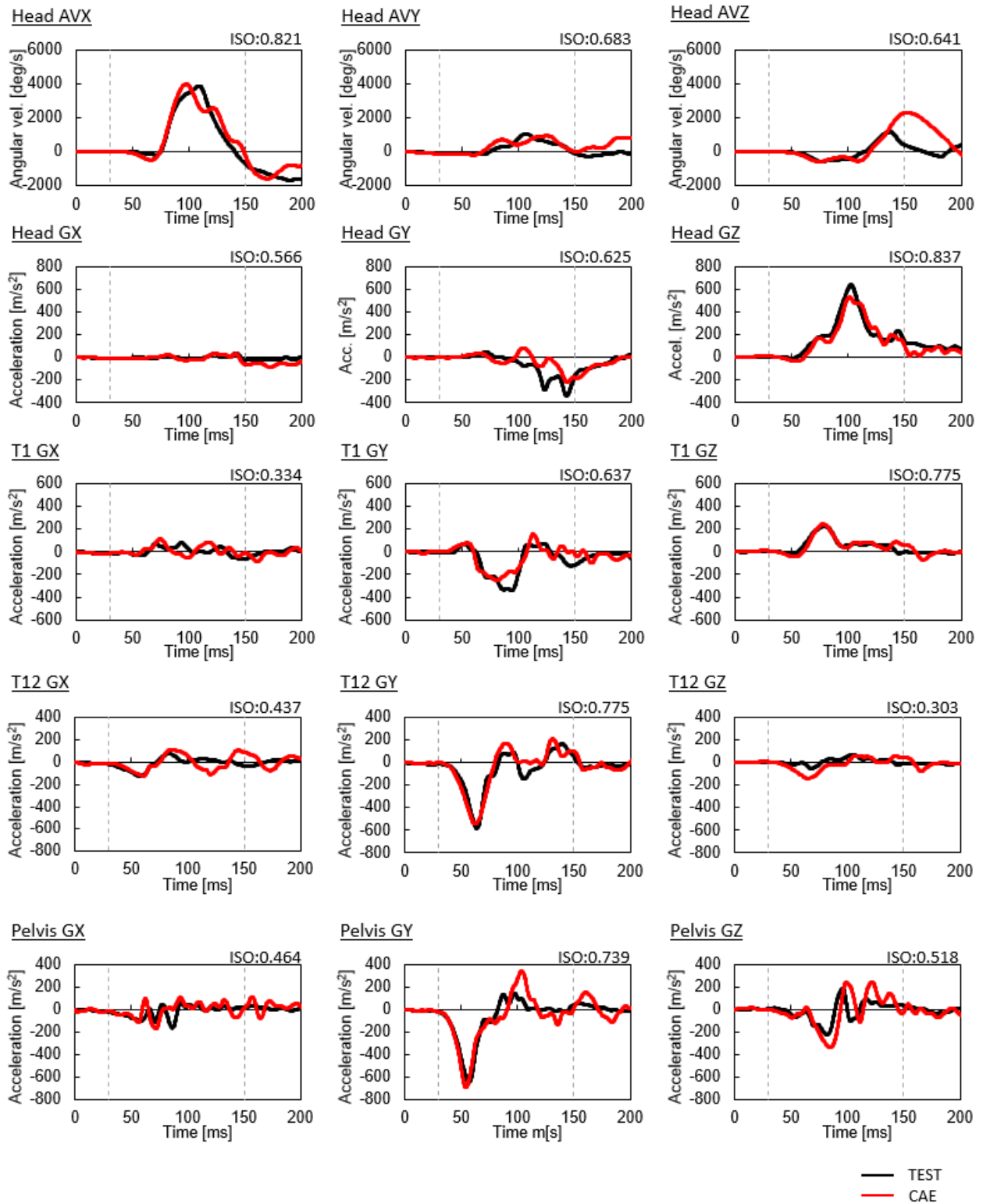


Fig. A2. Comparison of WorldSID time history sensor outputs (11 m/s).

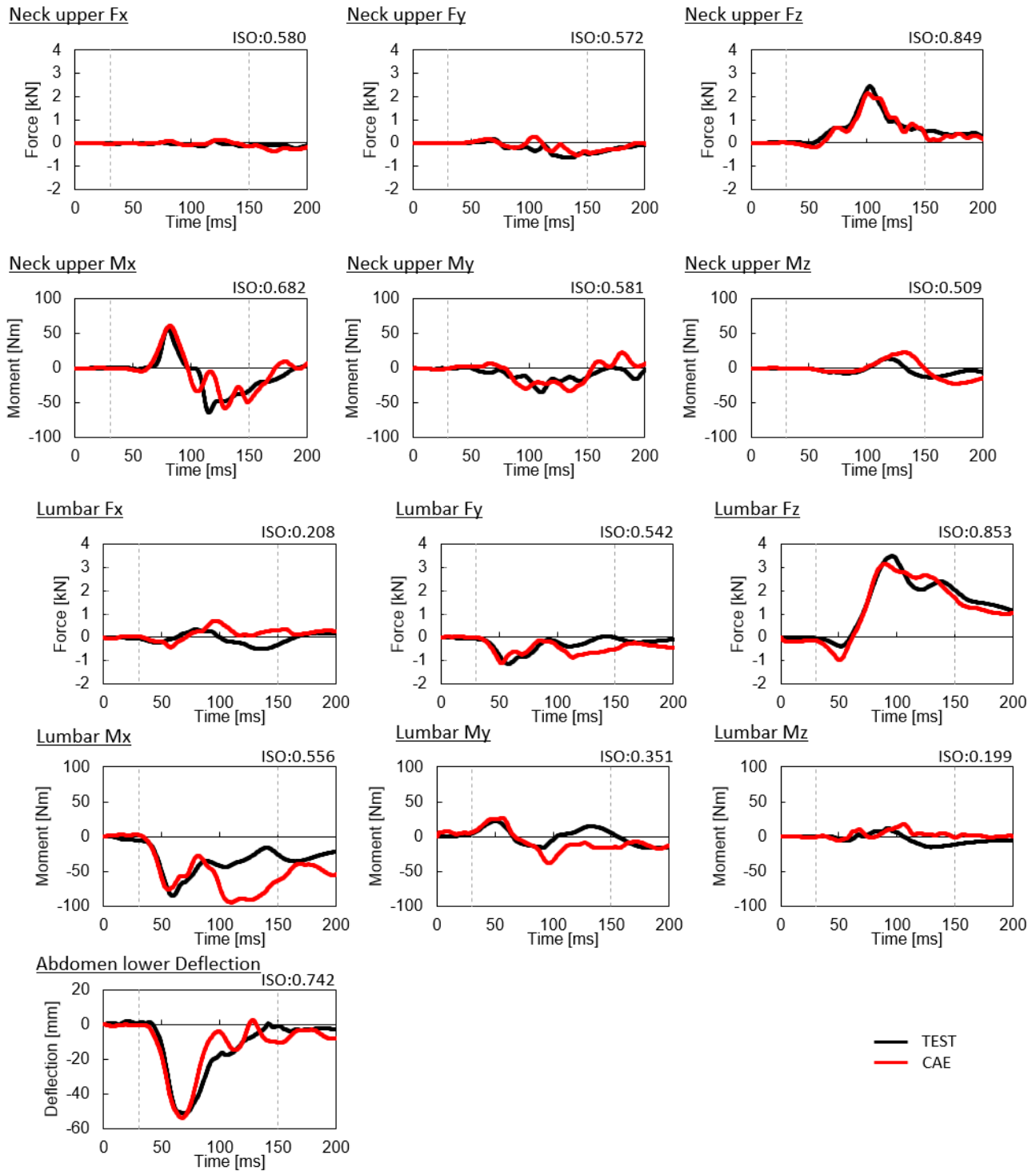
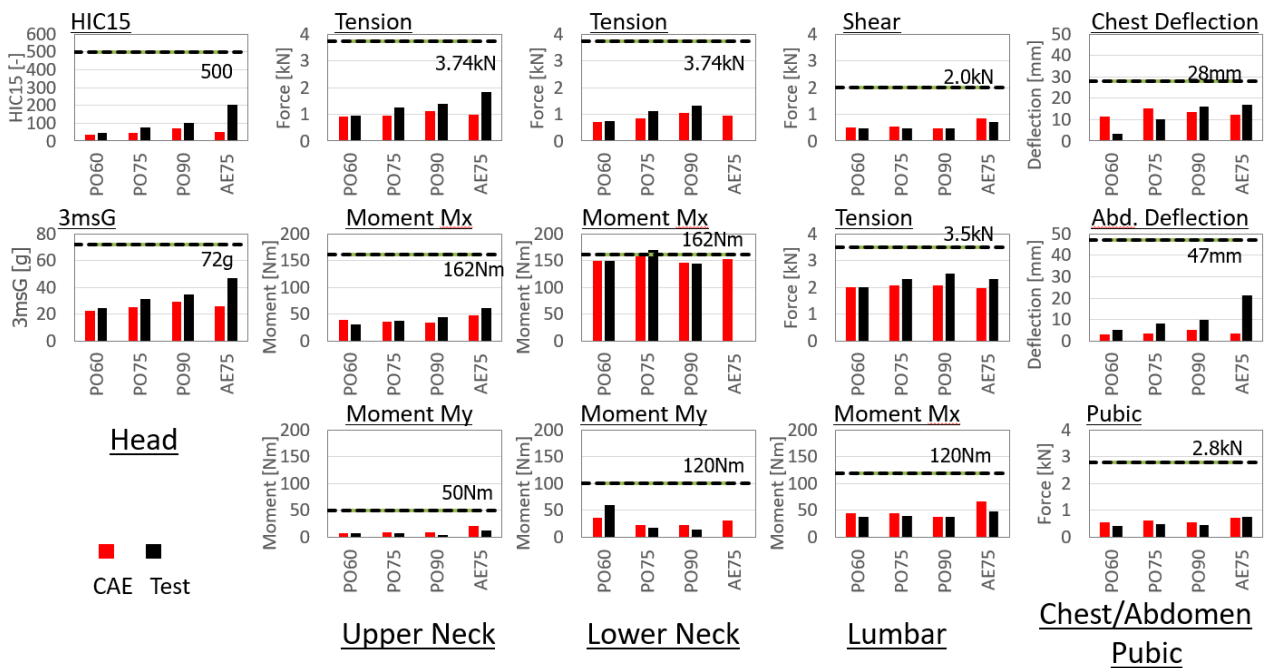


Fig. A2. Comparison of WorldSID time history sensor outputs (11 m/s).

B. Sled Model Validation of Injury Value Prediction using the WorldSID Model

Injury values of test results and CAE estimations were compared. The values were calculated using the filter class defined in Euro NCAP Technical Bulletin (TB021) [10]. Dotted lines in the graphs are low thresholds defined in the protocol.



Note: Lower neck sensor was not measured for AEMDB 75°

Fig. B 1. Comparison of Injury Values between Test and CAE

C. Comparison of Kinematics and Contact Force between the WorldSID and the THUMS

Figure C1. shows the occupant kinematics comparison between WorldSID (red line) and THUMS (blue line) of the head T1, T12 and pelvis in a front view at the time of the head reaching the maximum lateral movement with respect to the sled body of Pole 60°, 75°, 90° and AEMDB 75°. Furthermore, the front view of WorldSID and THUMS at the time of maximum lateral movement are shown in the list of their movements.

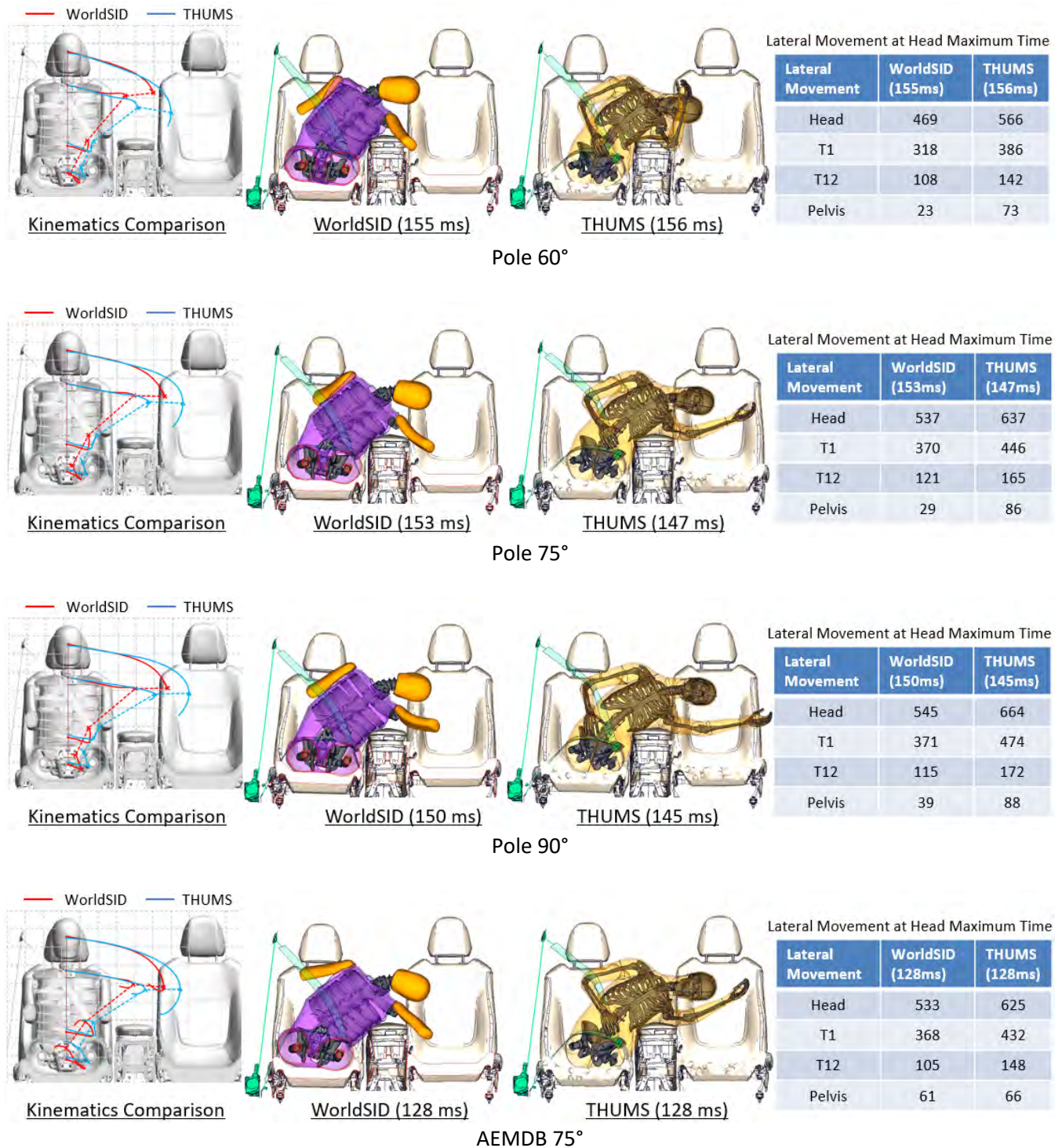
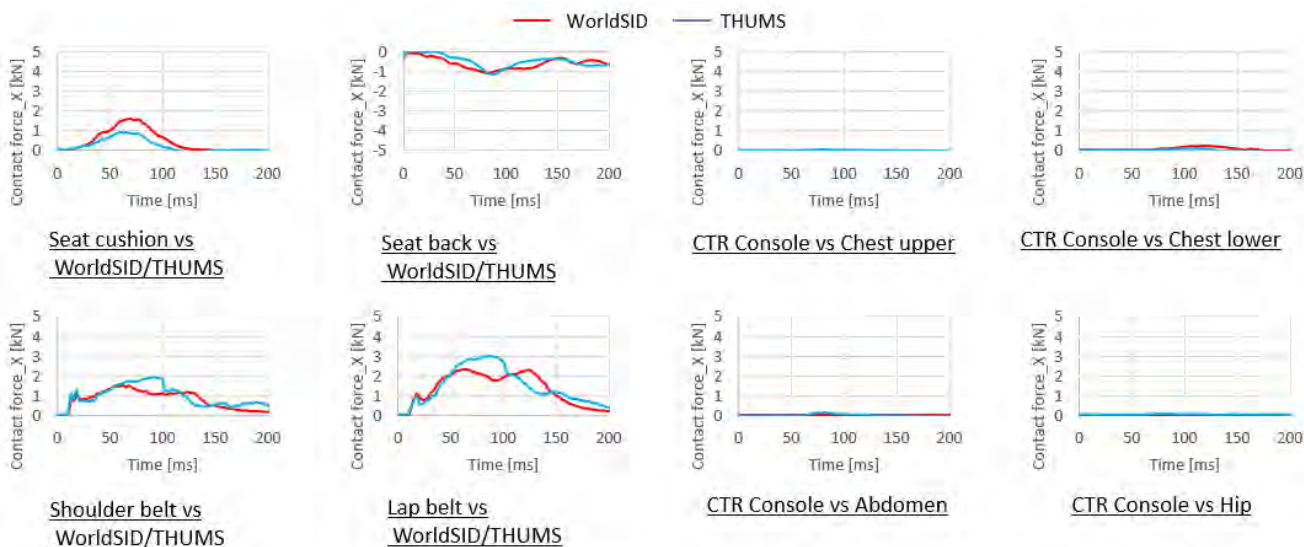
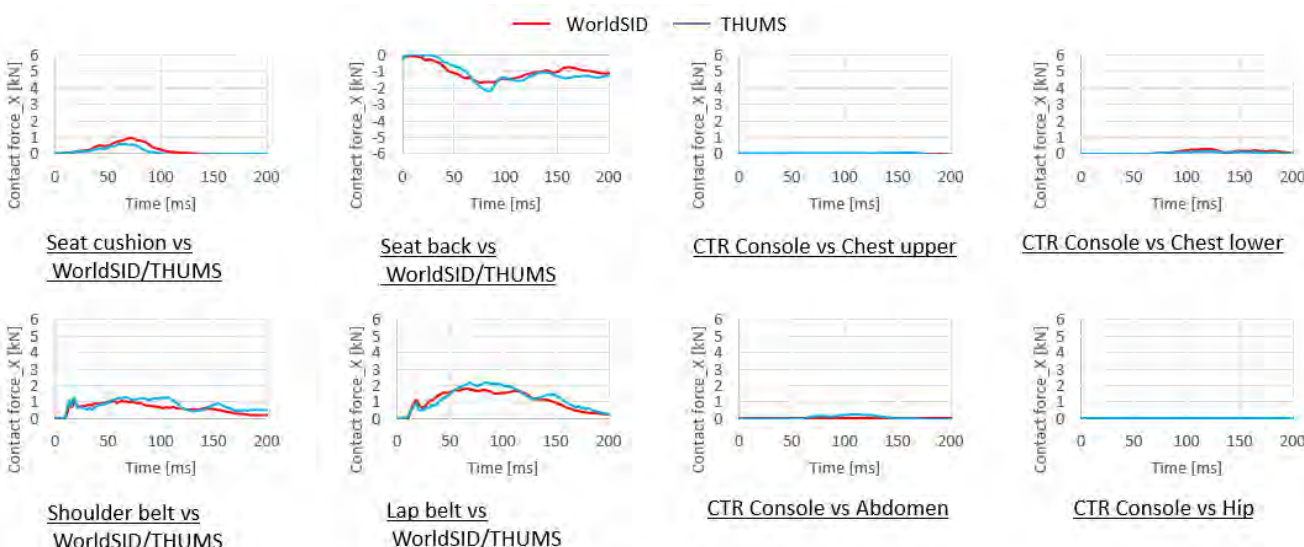


Fig. C1. Occupant kinematics.

Figure C2 X, Y, Z and R. shows comparison of contact force (X, Y, Z, Resultant) of Pole 60°, 75°, 90° and AEMDB 75° between WorldSID and THUMS.

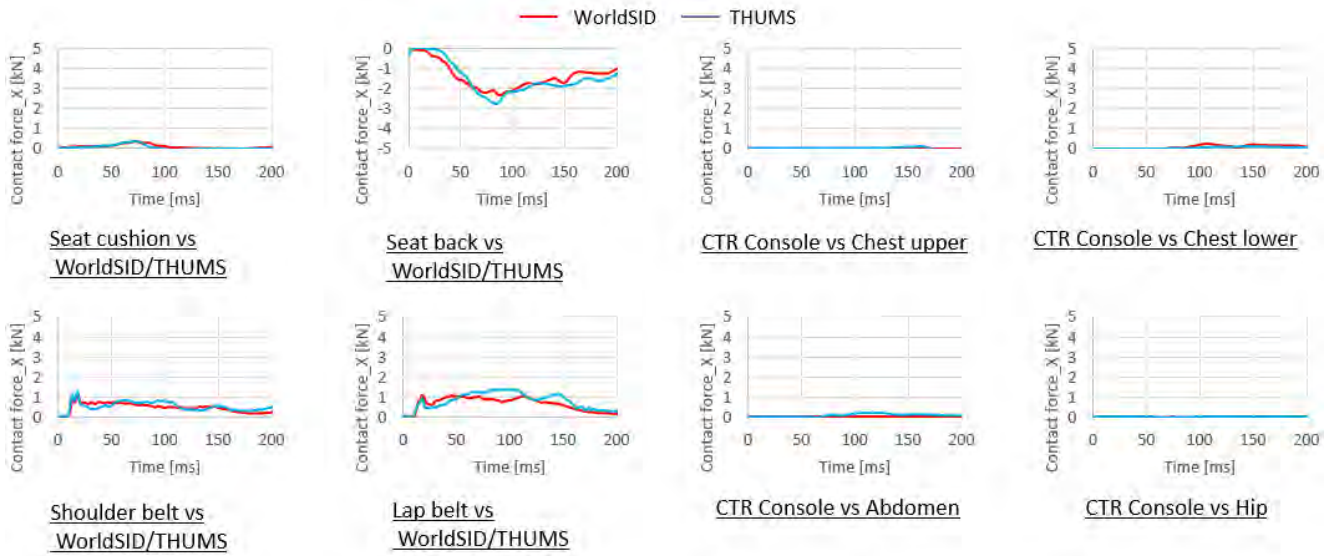


Pole 60°

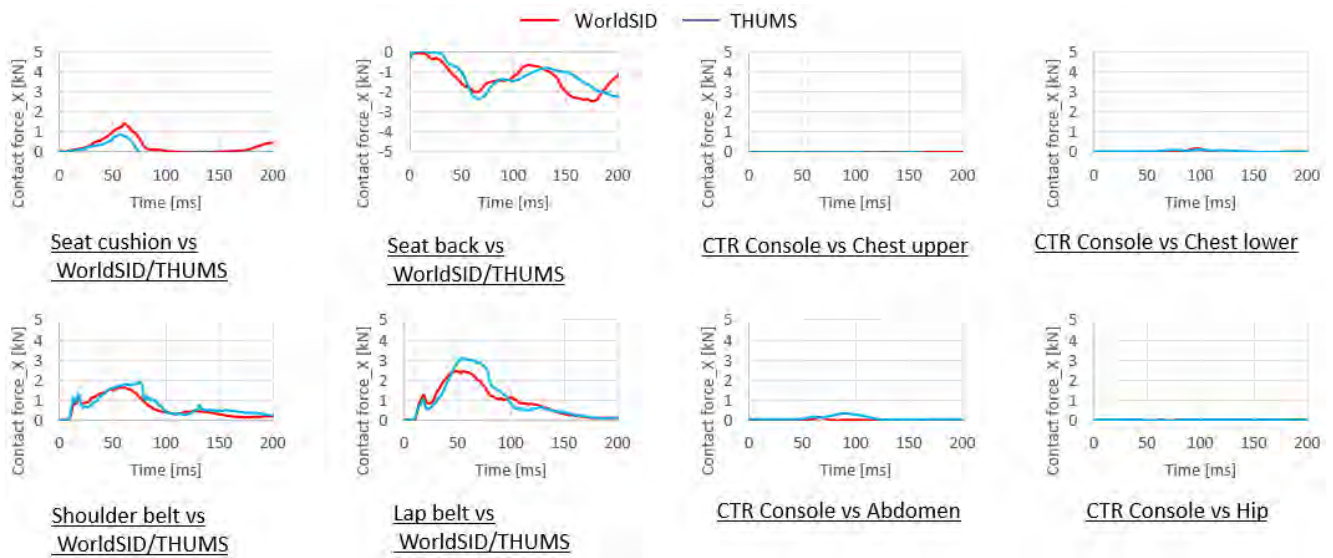


Pole 75°

Fig.C2 X. Comparison of Contact force (X) between WorldSID and THUMS

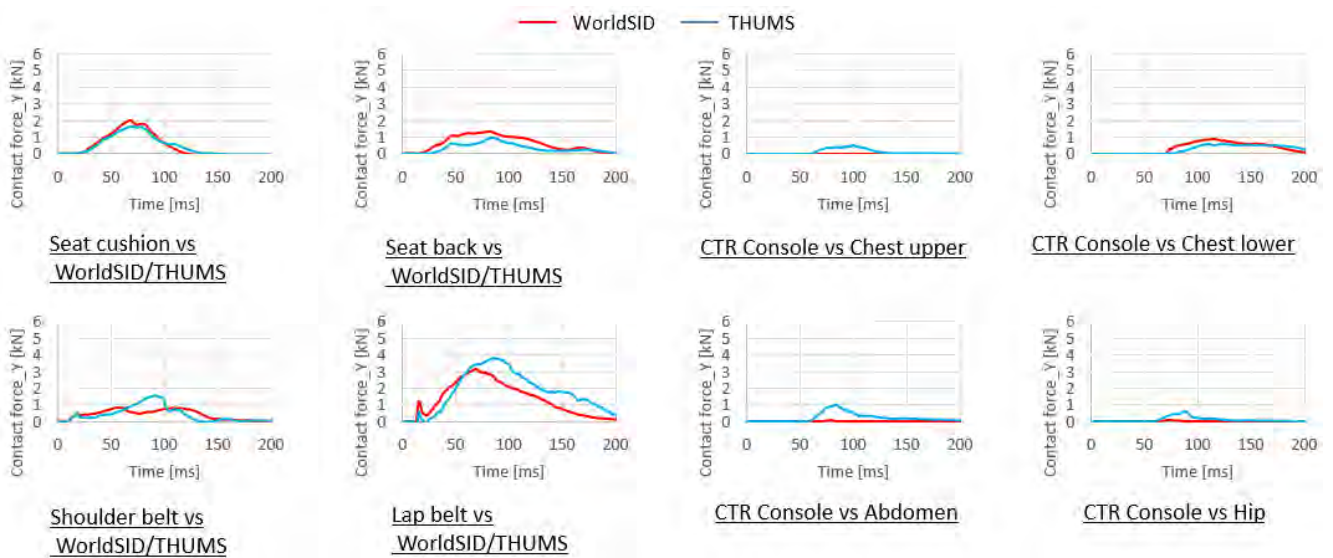


Pole 90°

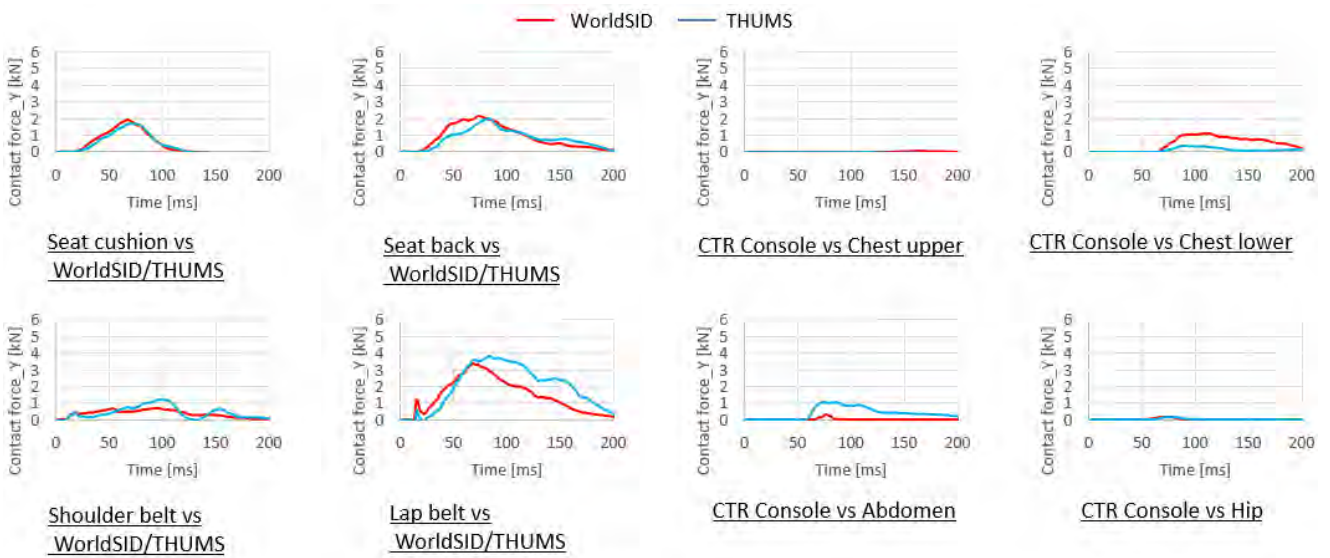


AEMDB 75°

Fig.C2 X. Comparison of Contact force (X) between WorldSID and THUMS

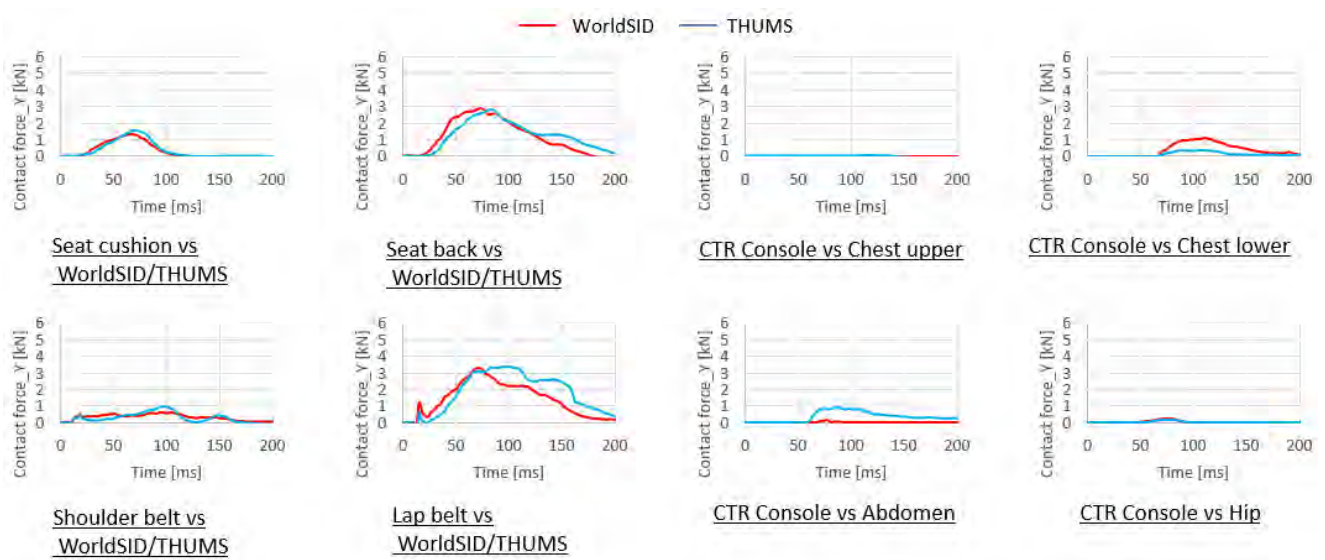


Pole 60°

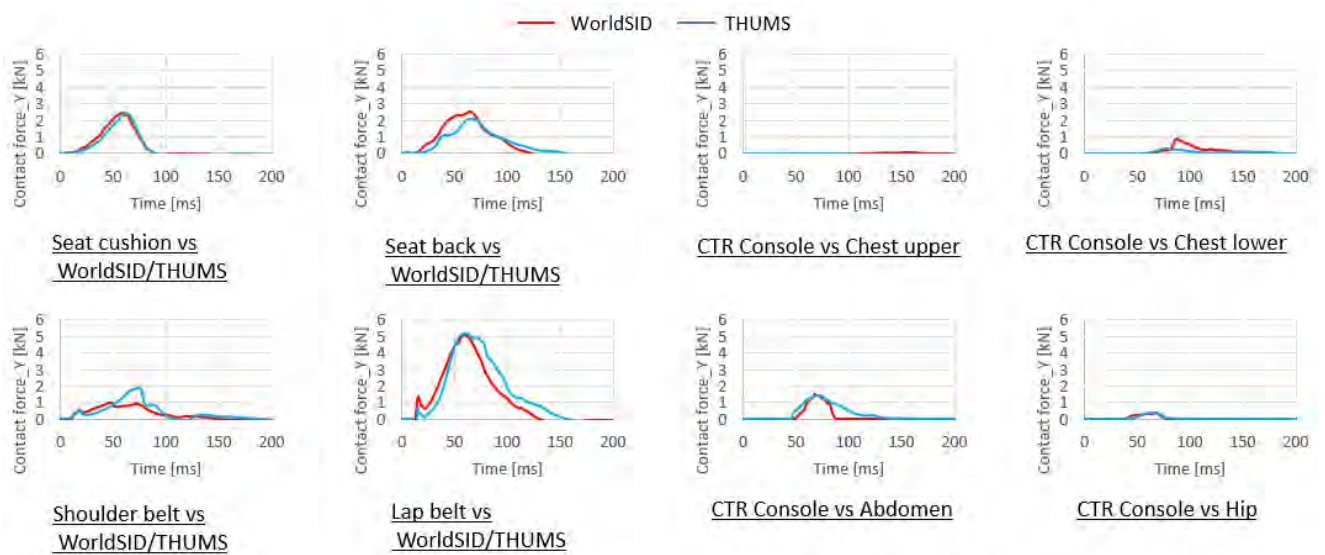


Pole 75°

Fig. C2 Y. Comparison of Contact force (Y) between WorldSID and THUMS

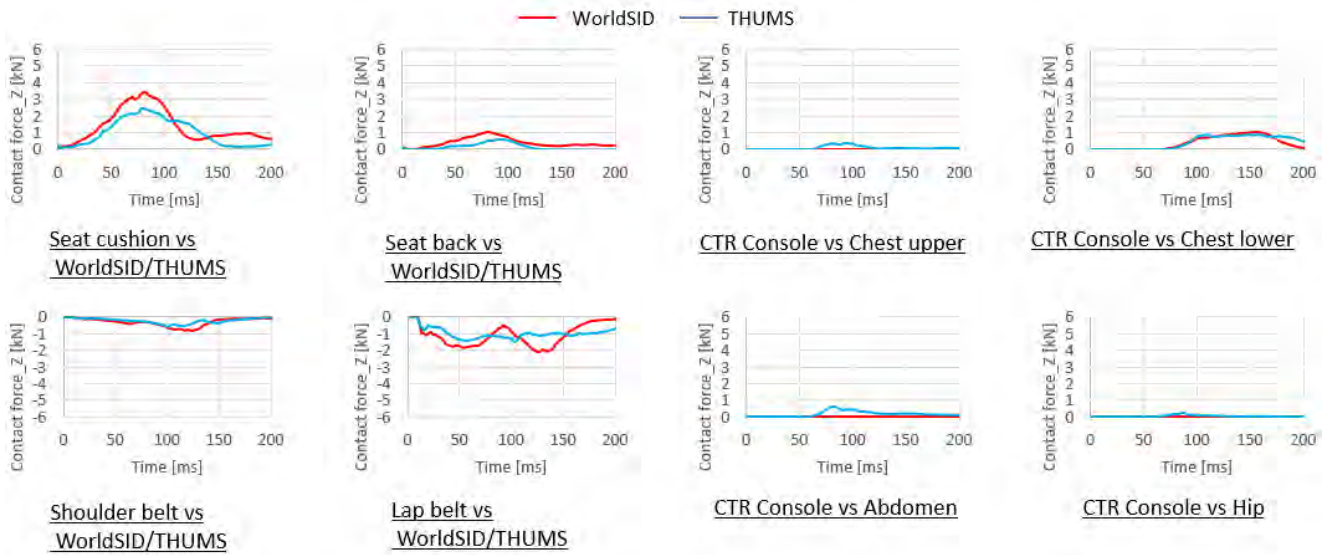


Pole 90°

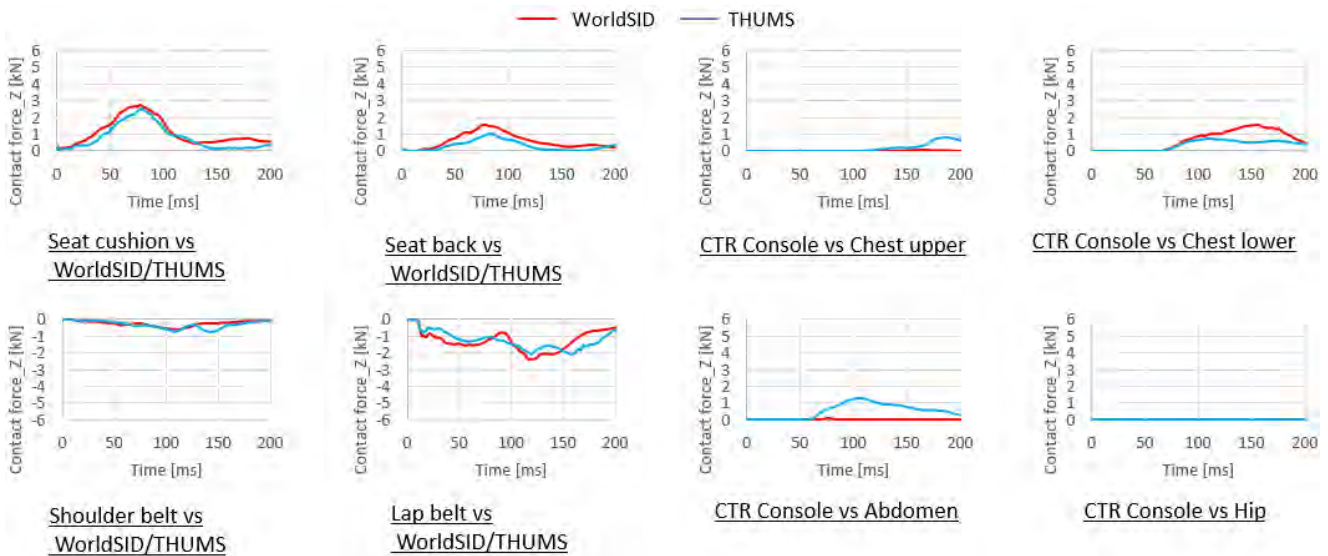


AEMDB 75°

Fig. C2 Y. Comparison of Contact force (Y) between WorldSID and THUMS

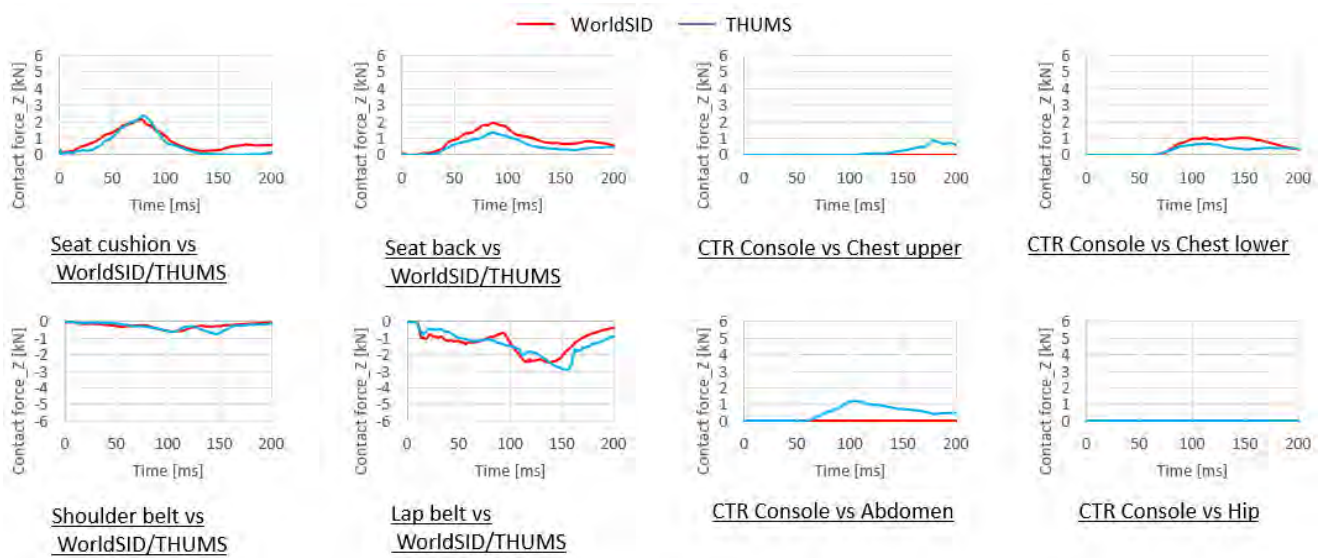


Pole 60°

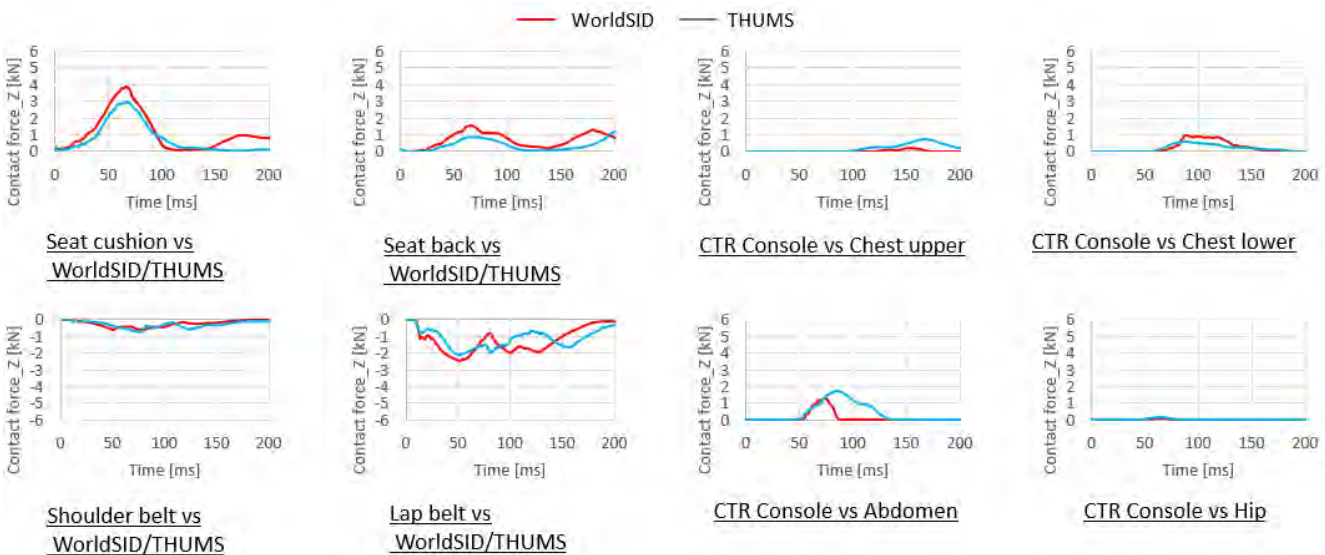


Pole 75°

Fig.C2 Z. Comparison of Contact force (Z) between WorldSID and THUMS

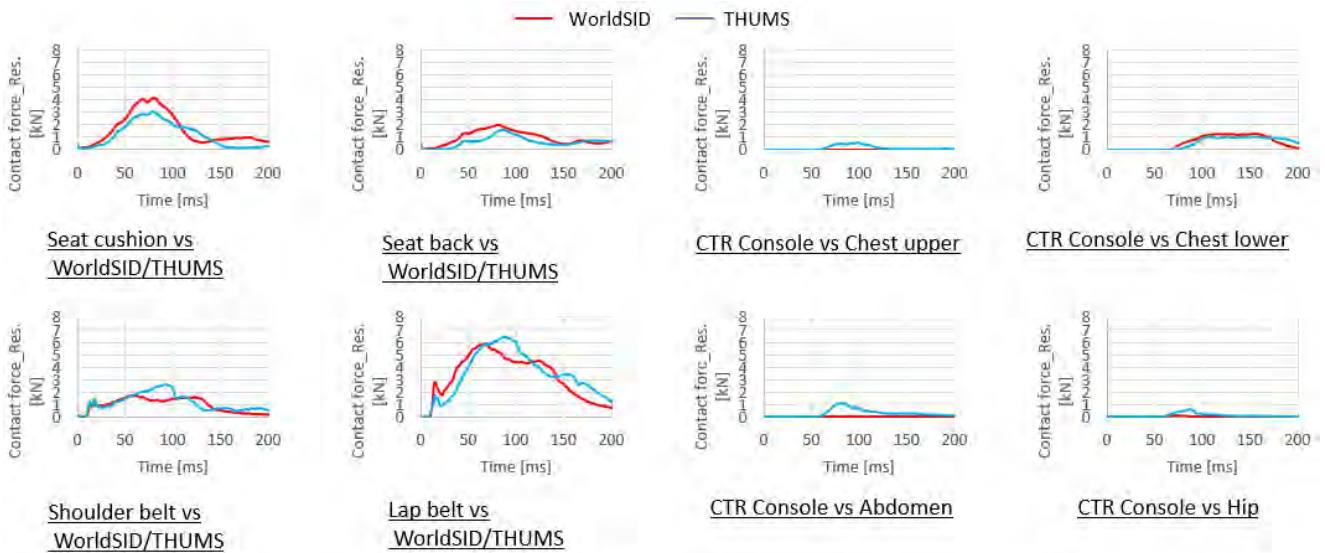


Pole 90°

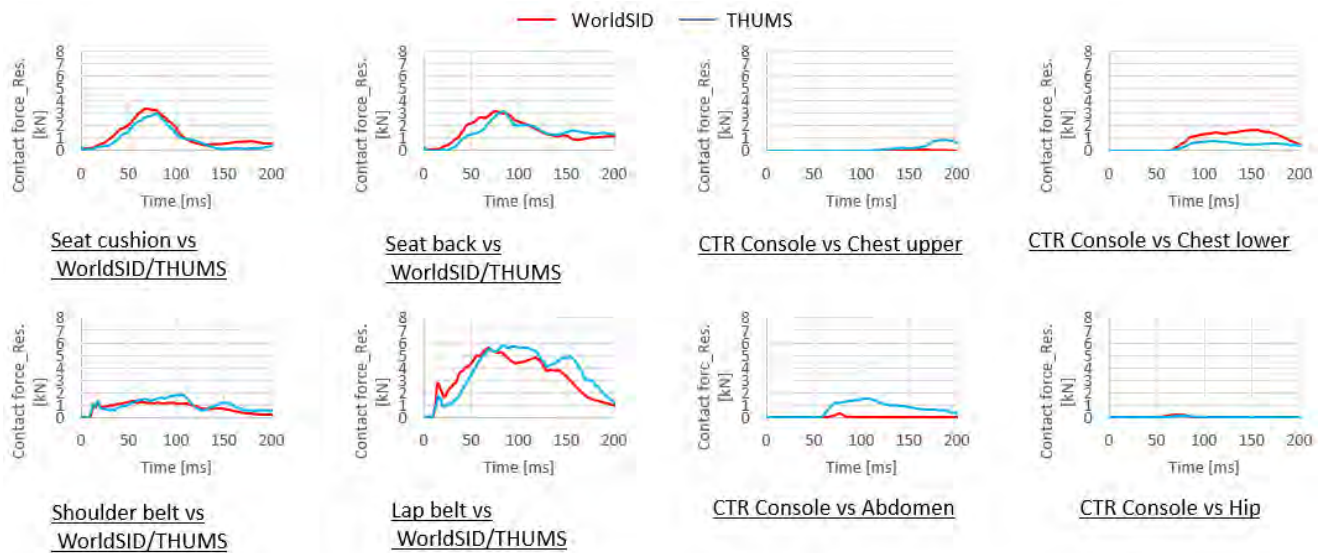


AEMDB 75°

Fig.C2 Z. Comparison of Contact force (Z) between WorldSID and THUMS



Pole 60°



Pole 75°

Fig.C2 R. Comparison of Contact force (Resultant) between WorldSID and THUMS

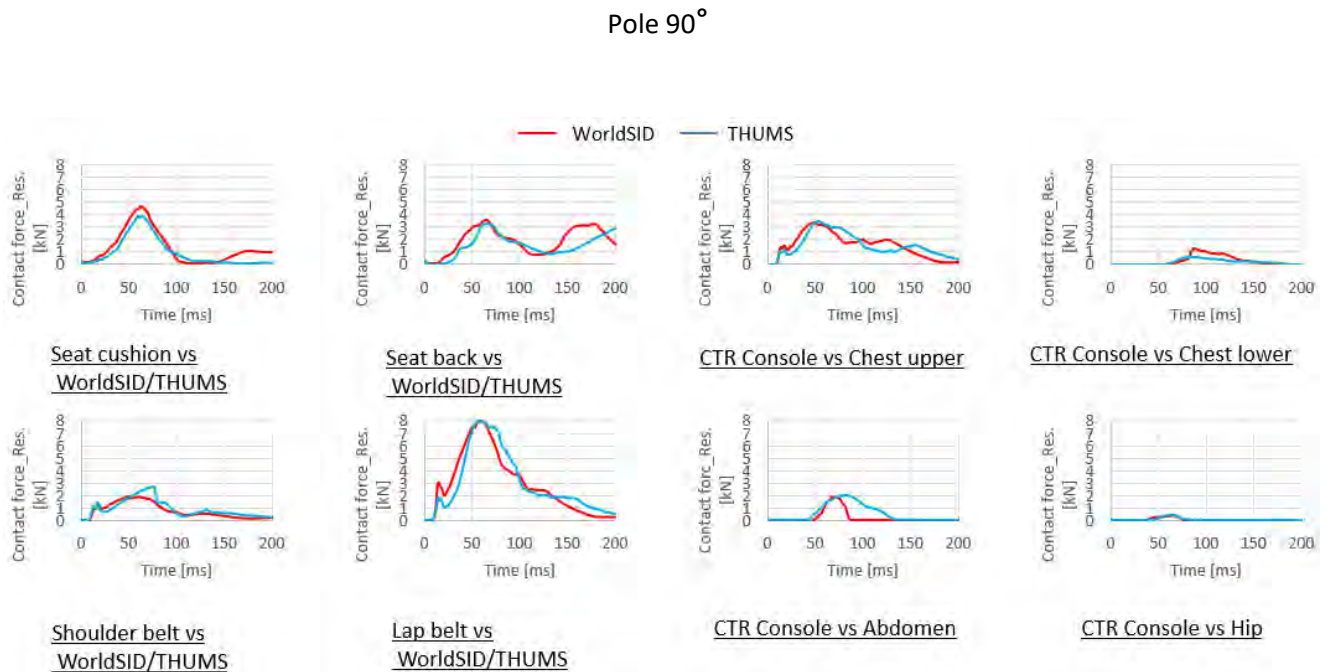
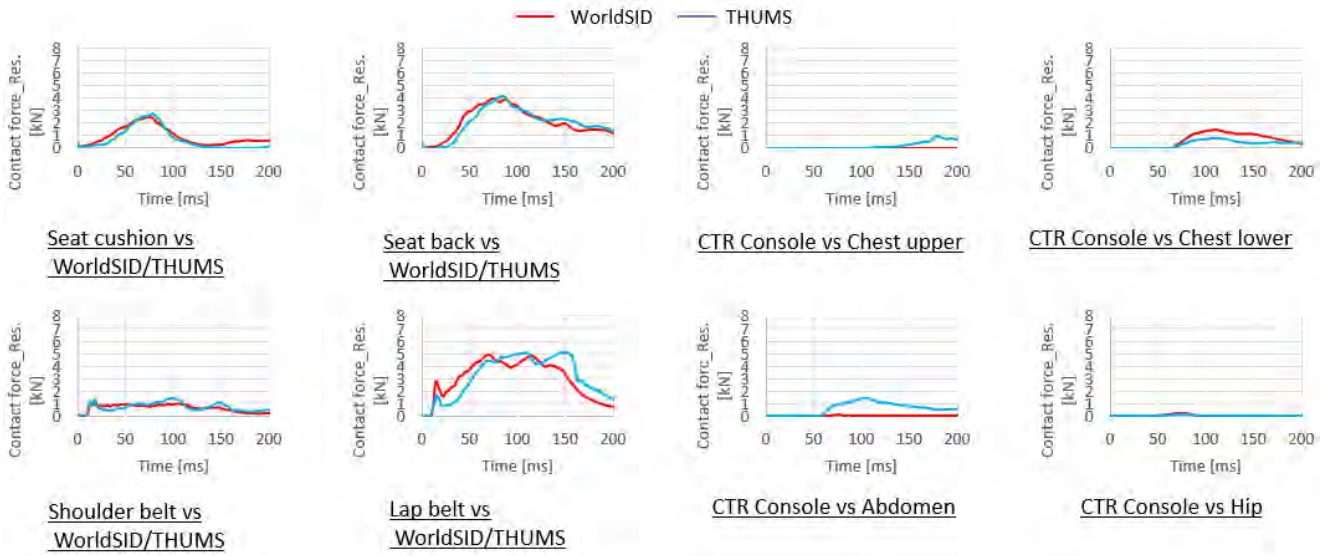


Fig.C2 R. Comparison of Contact force (Resultant) between WorldSID and THUMS

D. THUMS Rib Fracture Prediction

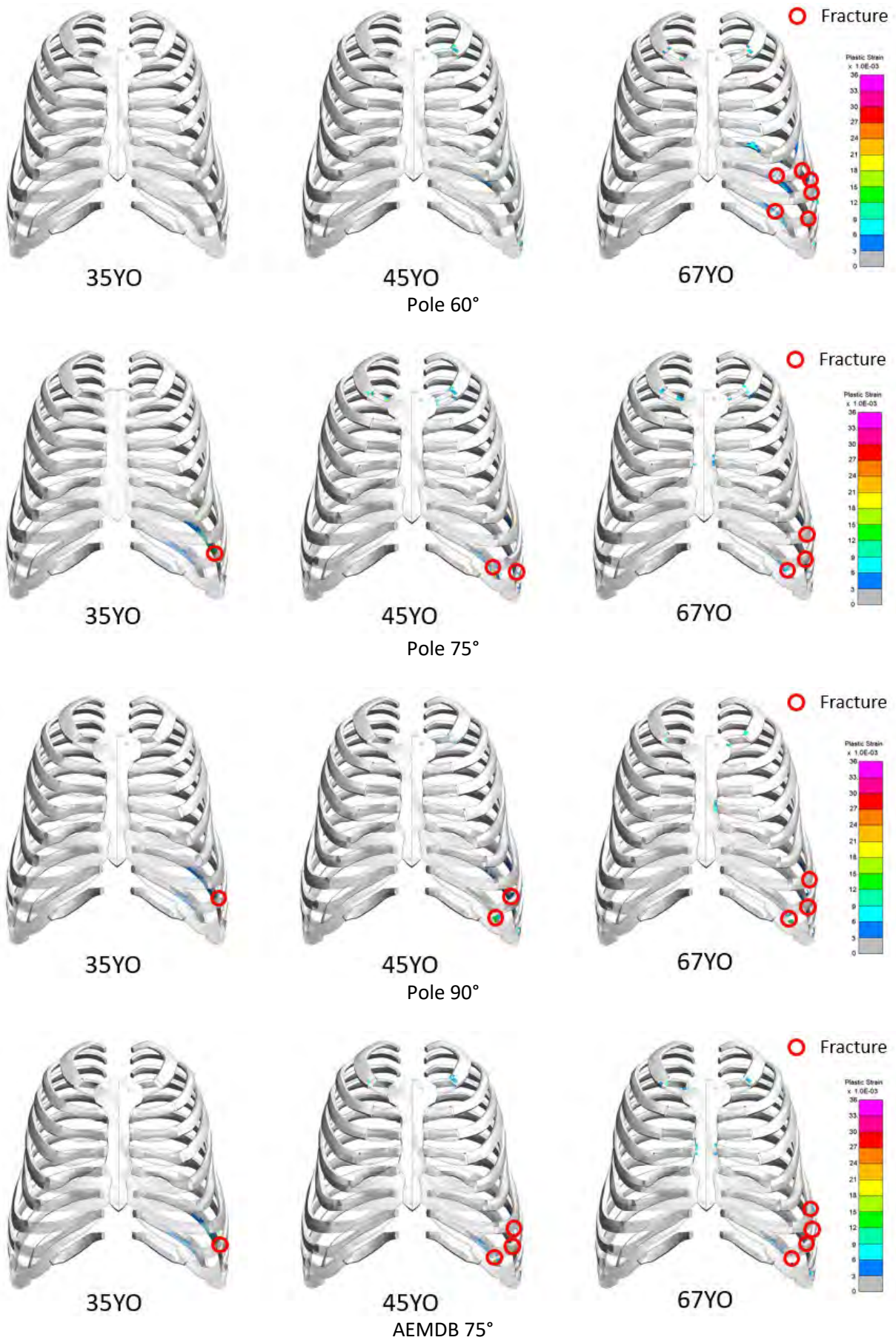


Fig. D. Rib Fracture prediction of THUMS